

The relative importance of selected factors controlling the oxygen dynamics in the water column of the Baltic Sea

S. Miladinova and A. Stips

CEC Joint Research Centre, Institute for Environment and Sustainability, Ispra (VA), Italy

Correspondence to: S. Miladinova (svetla.miladinova@jrc.ec.europa.eu)

Abstract

A 1-D biogeochemical/physical model of marine systems has been applied to study the oxygen cycle in four stations of different sub-basins of the Baltic Sea, namely, in the Gotland deep, Bornholm, Arkona and Fladen. The model consists of the biogeochemical model of Neumann et al. (2002) coupled with the 1-D General Ocean Turbulence Model (GOTM). The model has been forced with meteorological data from the ECMWF reanalysis project for the period 1998-2003, producing a six year hindcast validated with datasets from the Baltic Environmental Database (BED) for the same period. The vertical profiles of temperature and salinity are relaxed towards both profiles provided by 3-D simulations of General Estuarine Turbulent Model (GETM) and observed profiles from BED. Modifications in the parameterisation of the air-sea oxygen fluxes have led to a significant improvement of the model results in the surface and intermediate water layers. The largest mismatch with observations is found in simulating the oxygen dynamics in the Baltic Sea bottom waters. The model results demonstrate the good capability of the model to predict the time-evolution of the physical and biogeochemical variables at all different stations. Comparative analysis of the modelled oxygen concentrations with respect to observation data is performed to distinguish the relative importance of several factors on the seasonal, interannual and long-term variations of oxygen. It is found that natural physical factors, like the magnitude of the vertical turbulent mixing, wind speed and the variation of temperature and salinity fields are the major factors controlling the oxygen dynamics in the Baltic Sea. The influence of limiting nutrients is less pronounced, at least under the nutrient flux parameterisation assumed in the model.

1 Introduction

The Baltic Sea is a semi-enclosed and brackish sea, which together with other physical as well as socio-economic characteristics makes it very sensitive to anthropogenic pressures (Bonsdorff et al., 2001). Eutrophication remains the most pressing problem in the region, as nitrogen and phosphorous inputs are still high, despite considerable efforts to reduce discharges. Pulses of water streaming in at the bottom through the Danish straits transport salty and oxygen rich water from the North Sea into the Baltic Sea (Omstedt et al., 2004). The strong pulses are driven by special atmospheric forcing conditions, which cause large and long-lasting sea level differences between the Kattegat and the Western Baltic. Since the early 1980s, the Baltic Sea has experienced long-lasting stagnation periods with absence of strong pulses. Only in 1993 and 2003 such major inflows took place (Jakobsen, 1995; Feistel et al., 2003). Inflows from the North Sea are currently the principle source of oxygen in the deep water. The deepwater basins in the Baltic Proper suffer severely from long-term oxygen depletion. Oxygen deficiency has prevailed over very large areas. In the central Baltic Proper the oxygen concentrations are less than 2 ml/l at around a depth of 100 m, or even more shallow than that (HELCOM, 2003). At the same time, the area covered by hydrogen sulphide extends from the main eastern Basin of the Gotland towards the Northern Central Basin (Fig.1). Typically in August, oxygen is depleted in the bottom water of the Bornholm Basin and the western Gotland Basin. In the Arkona Basin the oxygen situation is good in the near-bottom water, although the level is lower compared to the long-term measurements. The oxygen conditions in the bottom waters of the Baltic Proper continues to be bad during 2003 - 2006 as well (HELCOM, 2007). The zones on the seabed with anoxic areas where hydrogen sulphide forms increase both in size and volume. More phosphorous consequently diffuses out of the sediments and into the deep waters of the Baltic.

Additional to the above mentioned horizontal advection of oxygen the principal natural physical factors affecting the concentrations of oxygen in the marine environment are temperature and salinity. Oxygen concentrations decrease with increasing temperature and salinity (Quinlan 1980). The other major factor controlling oxygen concentrations is the biological activity in the water and at the seafloor: photosynthesis producing oxygen and respiration and nitrification consuming oxygen.

Marine ecosystem models, which involve the interaction of physical and biogeochemical processes, are useful tools for assessing and predicting the trends in oxygen variation and for identifying the areas more susceptible to oxygen deficiency. These models should take into account the most important biogeochemical processes and the physical control of the ecosystem driven by advection and diffusion. Efficient models of marine systems can simulate the seasonal evolution, inter-annual variability and spatial heterogeneity across the range of coastal and eutrophic situations with little or without re-parameterisation. Although the usual way to develop such models is to couple circulation models with biological models, simplified model systems based on 1-D water column models (e.g. those of Burchard et al., 2006; Kühn and Radach, 1997; Blackford et al., 2004) are very helpful tools for model development. Depending on the scientific question, they can be also reliable in studying marine ecosystem dynamics of coastal marine areas.

The present study aims to assess the relative importance of different factors controlling the oxygen cycle in the water column of the Baltic Sea by the use of a 1-D water column model. Thus, the relative importance of following factors is investigated in detail:

- the significance of the principal hydrographic situation is studied by comparing several stations with very different hydrographic characteristics;
- the importance of the accuracy of hydrographic characteristics (temperature/salinity structure) - by comparing simulations relaxed with measured profiles and 3-D model results;
- the effect of the vertical turbulent exchange - by varying the parameters of the turbulence model;
- the influence of the atmospheric forcing – by multiplying the wind speed by a factor from the interval [0.5;1.5];
- the importance of the parameterisation of the air-sea oxygen exchange - by analysing the impact of different available parameterisations;
- the relative importance of limiting nutrients.

The study is organized as follows. In Sect. 2 we describe briefly the 1-D model and characterise the type of the method used to model the system, while in Sect. 3 we provide the model setup and forcing. Section 4 shows the effect of the air-sea oxygen parameterisations on the surface oxygen dynamics. In Sect. 5 are presented model results at different stations

and comparisons between observations and model results. The model sensitivity analysis is presented in Sect. 6. The last section includes a discussion and some conclusions.

2 Model description

We use the coupled 1-D ecosystem model of Burchard et al. (2006) to simulate the oxygen and nitrogen cycles in some selected stations of the Baltic Sea. As a physical part of the 1-D ecosystem model the GOTM (General Ocean Turbulence Model, www.gotm.net) is applied. The turbulence is modelled with a two-equation turbulence model; one equation for the turbulent kinetic energy and one equation for the dissipation rate of the turbulent kinetic energy. The model includes a simple parameterisation of deepwater mixing. In order to parameterise unresolved turbulence production by internal wave shear, internal wave breaking or Kelvin–Helmholtz instability under stably stratified conditions, a lower limit to the turbulent kinetic energy is set ($k_{\min} = \text{const}$). We have found that from the large number of well-tested turbulence models implemented in GOTM, the κ - ε model is a very appropriate tool to model the dynamical vertical structure and the actual turbulent diffusive vertical transport in some Baltic Sea stations.

A biogeochemical model of medium complexity (ten state variables) is used in this study (Neumann, 2000; Neumann et al., 2002). This model is of Eulerian-type, so all state variables are expressed as concentrations, no matter whether they are dissolved chemicals (e.g. nutrients, oxygen) or particles (e.g. phytoplankton cells). For example, the ERSEM (European Regional Seas Ecosystem Model, Baretta et al., 1995) is an Eulerian-type model of higher complexity. In the model, the oxygen utilisation and production is connected with nitrogen conversation. The oxygen concentration controls processes as denitrification and nitrification. If oxygen is depleted, than nitrate is used to oxidize detritus, and if nitrate vanishes sulphate is reduced to hydrogen sulphide. Hydrogen sulphide is accounted for as negative oxygen concentrations ($2\text{H}_2\text{S}=\text{O}_2$). Reduction of nitrate (denitrification) is counted as a loss of nitrogen in the model. In detail, the state variables are: ammonium, nitrate, phosphate, flagellates, diatoms, blue-green algae, detritus, zooplankton, oxygen and sediment detritus.

The model of Neumann et al. (2002) has been recently coupled to the physical model as BIO_IOW module of the GOTM package. The GOTM-BIO_IOW model has been tested by Burchard et al. (2006) for the Gotland station (BY15) with water depth of about 250 m. The comparisons between model results and observation data from COMBINE program (under

the umbrella of HELCOM) for the period 1983-1991 show that the hindcasting of interannual variability of nutrients nitrate and phosphate, and phytoplankton is not satisfactory. Burchard et al. (2006) found that the κ - ε model predicts too shallow mixed layers in the Baltic Sea when applied without limitation of turbulent kinetic energy, $k_{\min}[m^2/s^2]$. It is illustrated that the parameter k_{\min} can act as a tuning parameter of the model (Burchard et al., 1998; Burchard et al., 2006). However, more complete and accurate studies of model sensitivity analysis and/or model skill assessment have not been reported.

The validity of a 1-D approximation in the Baltic Proper is confirmed also by some other model results (Vichi et al., 2004; Omstedt and Axell, 1998; Stigebrandt, 1987). They are mainly related to periods, when advection is negligible (so-called stagnant periods). Despite, that a 1-D model exhibits limitations in simulating seasonal and interannual variability of the deep water mixing and the formation of density currents (Axell, 2001), it is a good tool for basic studies, improving the model parameterisation and investigation of some system properties.

3 Model forcing and setup

The model is run for a six year period, from January 1, 1998 to December 31, 2003 and the initial profiles are approximated from available oceanographic measurements. The simulation period includes stagnant (1998-2002) and fluctuant (2003) periods. The only major inflow to the Baltic Sea during the investigated period was in 2003 (Feistel et al., 2003). However, several inflows of less strength occurred during the period (Matthäus and Nausch, 2003).

Depth profiles of temperature and salinity along with surface meteorological data and nutrient components are used to force the model. The meteorological forcing data are taken from the ECMWF (European Centre for Medium Range Weather Forecast, www.ecmwf.int) data server (ERA-40 re-analysis data). The frequency of meteorological data is six hours. Data sets of temperature, salinity, concentrations of oxygen and chlorophyll a are extracted from the Baltic Environmental Database (BED) via internet based software NEST (<http://nest.su.se/bed>). The initialization of some initial parameters of the BIO_IOW module is done by the use of BED data, as well. Finish Institute of Marine Research (FIMR) Baltic Sea monitoring data (http://www.fimr.fi/en/tietoa/helcom_seuranta/en_GB/bmp/_data) is also used for model verification. The water transparency of Baltic Sea, measured as Secchi depth,

has been thoroughly estimated in the report of Laamanen et al. (2004) and it is assumed to be 5 m in our calculations.

Nutrient fluxes at the air-sea surface have been adjusted in order to parameterise lateral nutrient fluxes which are neglected in the 1-D model. Thus, much higher values than the real ones are used in calculations. In order to highlight the differences between the physical conditions at the studied stations, we fix the surface fluxes and initial concentrations of ammonium, nitrate, and phosphate for all numerical simulations. The estimation of the nutrient values is done on the base of sensitivity analysis. Statistical and graphical techniques are applied to compare quantitatively the multiple executions of the model (Sect. 6.4).

The computed temperature and salinity profiles have been relaxed towards observed profiles (BED data) or profiles calculated with GETM model (www.getm.eu, Stips et al. 2005). The optimal relaxation time is about 5 days. The model is run using a two year repeating cycle of forcing data for 1998 as a ‘spin-up’ period in order to achieve a quasi-equilibrium state and obtain reasonable initial conditions.

4 Improvement of the model

In this section we discuss the effect of parameterisation of the air-sea exchange on oxygen dynamics. The oxygen exchange with the atmosphere is usually described by

$$F = V (O_{sat} - O), \quad (1)$$

where F [$g O_2 / m^2 d$] is the air-sea oxygen flux, V [m / d] is the transfer (piston) velocity, O and O_{sat} [$mmol O_2 / m^3$] are surface and saturation oxygen concentrations, respectively. In the BIO_IOW module the piston velocity is assumed as a constant ($V = 5$ [m / d]) and the saturation oxygen concentration is calculated by

$$O_{sat} = a_1 - a_2 T_s, \quad (2)$$

where T_s is the surface temperature and a_1, a_2 are constants (Neumann et al., 2002; Burchard et al., 2006). First, we have implemented the model for the station BY15 in the central Gotland Sea. In Fig. 2 a, b are shown the surface temperature and oxygen time series, respectively. The model is in a good accordance with the data over the full six year period, especially in describing the seasonal variability. However, it captures the variation only with

lower amplitudes of surface oxygen concentrations during summer (Fig. 2b). The difference between simulated and observed surface concentrations of oxygen is more pronounced during summer of 1999, 2001-2003 when the surface temperature reaches about 23 C° (Fig. 2a). This discrepancy is due to an overly simplified computation of the oxygen surface fluxes. So, we have modified the parameterisation of the surface oxygen flux in the BIO_IOW module.

In this paper, the piston velocity is calculated by the model of Liss and Merlivat (1986), which includes three regimes (smooth surface, rough surface and breaking waves) depending on the magnitude of wind speed, w :

$$\begin{aligned}
 \text{at } w < 3.6 \text{ [m/s]:} & \quad V = 1.003 w / Sc^{0.66} \\
 \text{at } 3.6 \leq w \leq 13 \text{ [m/s]:} & \quad V = 5.9(2.85 w - 9.65) / Sc^{0.5} \\
 \text{at } 13 < w \text{ [m/s]:} & \quad V = 5.9(5.9 w - 49.3) / Sc^{0.5}
 \end{aligned} \tag{3}$$

The Schmidt number Sc is defined as ratio between the kinematic viscosity and the molecular diffusivity of oxygen. We have applied the following expression for Sc (Stigebrandt, 1991)

$$Sc = 1450 - 71T_s + 1.1T_s^2. \tag{4}$$

Equation 4 is valid in the interval $0 < T_s < 40 \text{ C}^\circ$ and thus, it is applicable in the case of a non-freezing sea surface. Instead of the linear dependence of O_{sat} on temperature involved in the BIO_IOW module, we have used the formula of Weiss (1970). For comparison, in Fig. 2c is shown the considerably improved surface oxygen evolution of the above described test case at BY15 after running the modified BIO_IOW module.

In order to investigate in detail the effect of the parameterisation of the air-sea exchange on the surface oxygen dynamics, we consider four cases with different parameterisation of the air-sea exchange and a case without phytoplankton growth and grazing (Table 1). The mean absolute error (mean value of the absolute differences between simulated and measured values) represents the magnitude of the difference between the BED observation data and our numerical simulations, while the linear correlation coefficient, R , measures the strength and the direction of a possible linear relationship between them. The root mean square difference (RMSD [mlO_2/l]) of simulated and measured surface oxygen concentrations is also given in Table 1. It measures the size of discrepancies between simulated and observed values. A complete description of the above mentioned statistics can be found in Taylor (2001) among other sources. The statistics are calculated on the basis of the available measurements of the

surface oxygen content during the studied six year period at the station BY15 and the corresponding simulated values. As shown in Table 1, in case I (constant piston velocity and linear oxygen saturation) both mean absolute error and RMSD reach the highest values, while the correlation coefficient has the lowest value. We have found the best agreement with the observation data in case IV (new piston velocity and nonlinear oxygen saturation). The improvement is caused approximately to the same amount by both new piston velocity and new nonlinear oxygen saturation, as can be seen from Table 1 (please compare case II (only nonlinear oxygen saturation) and case III (only new piston velocity)). It is worth to note, that even without any primary production (case V) the improved model predicts reasonable surface oxygen concentrations that are better than in the case with a linear dependence of O_{sat} on temperature and constant piston velocity (case I). This suggests that the parameterisation of the air-sea oxygen exchange has a major effect on the surface oxygen dynamics.

5 Model results and validation

The strong density stratification in the Baltic Sea suppresses vertical mixing of the water and the transport of oxygen from the surface to the bottom. During very exceptional conditions when the inflow lasts long enough (over two weeks) saline water from the North Sea can reach far enough into the Baltic Sea. The saline water is only very slowly mixed with Baltic Sea water and it flows through the Arkona and Bornholm basins in about six months, then to the central basin of the Baltic Sea, the Gotland deep, replacing the old Baltic Sea water, often containing little or no oxygen but some hydrogen sulphide (Feistel et al. 2003). The medium-strength inflows are important as well because they have potential to renew intermediate layers of the Baltic Proper halocline (Feistel et al. 2006). Since one of our purposes is to explore the influence of the principal hydrographic situation on the oxygen cycle in the water column of the Baltic Sea, we simulate the oxygen and nitrogen cycles at several stations with very different hydrographic characteristics. For a detailed presentation, we selected four stations with a quite different location in the Baltic Sea, namely:

Gotland (249 m depth), a very deep central station BY15 (20E, 57.3N) of the Baltic Proper, with limited water exchange, with a well-mixed surface layer and salinity stratified deeper layer;

Bornholm (91 m depth), a central station BY5 (15.9E, 55.2N) of the Bornholm basin, with limited water exchange, with a well-mixed surface layer and salinity stratified deeper layer;

Arkona (47 m depth), a central station BY1 (14E, 55N) of the Arkona basin, a shallow station strongly influenced by the pulses of saline and oxygenated water from the Kattegat;

Fladen (80 m depth), a station BY0 (11.5E, 57.3N) of the Kattegat basin, close to the North Sea, with the highest salinity among our selected stations.

Each of the first three stations might be considered as a representative station for the corresponding basin (Reissmann, 2006). The regional characteristics of the salinity, potential temperature and oxygen content are represented well by the hydrographic measurements in the corresponding central stations.

5.1 Water column structure

The annual temperature variation in the surface water of the Baltic Sea is great, having differences of up to 20°C. For example, in Fig. 2a is shown the surface temperature at station BY15. The surface temperature at BY5 behaves in the same way like that at BY15, while the bottom one is approximately constant (7°C) at both stations (it decreases to 3°C only after the inflow of 2003). At BY5 the surface salinity is about 7.5 PSU (7 PSU at BY15) and the bottom salinity varies slightly between 15 and 17.5 PSU (12 and 13 PSU at BY15) and reaches a peak of 19.2 PSU after the inflow in 2003. A halocline separates the lower saline surface water, 6-9 PSU, from the more saline deep water, 15-20 PSU, (for all stations except for BY0, where the surface salinity varies between 16 and 30 PSU and the bottom one between 33 and 35 PSU) and excludes the deep water from vertical mixing. The halocline begins at a depth of about 10-20 m in the Fladen station, 30-40 m in the Arkona basin, 35-50 m in the Bornholm basin, and 60-70 m in the Gotland basin (IOW, 2003; Wasmund et al., 1998).

For illustrating the seasonal cycle of the density stratification, in Fig. 3 is shown the comparison between the simulated and observed density difference, $\rho_t = \rho_b - \rho_s$ [kg/m^3] (where ρ_b and ρ_s are the bottom and surface density, respectively) at BY5. It particularly indicates the less stratified winter period and the presence of more stable conditions in

summer (Lass et al., 2003; Mohrholz et al., 2006; Sellschopp et al., 2006). The variability of ρ_t is simulated quite well, because of the applied salinity relaxation.

In summer, additionally a thermocline forms at about 15-20 m depth and the temperature of the intermediate water between thermocline and halocline usually remains the same as during winter (4-10°C). The thermocline exists until October, then in the autumn the surface water starts cooling and sinking until it reaches the temperature of maximum density. The thermocline and the related density differences in the upper layer disappear and finally wave and wind actions mix the whole layer above the halocline.

The vertical oxygen distribution at BY5 is shown in Fig. 4 for selected representative days during the year 2001. It is nearly constant in the layer above the halocline except for the summer months. Moreover, the concentrations of oxygen are higher in the layer below the thermocline (cold intermediate layer) than in the other water layers. In the halocline oxygen decreases rapidly, so the halocline acts as a barrier for oxygen transport into the deeper waters.

Thus, one can distinguish three main layers of the sea water column at BY5, as well as at the other three stations:

- surface (mixed) layer, where the temperature, the water salinity and the oxygen concentrations are more or less vertically constant;
- intermediate layer (the depths below thermocline till the end of halocline), where the temperature, the water salinity and the oxygen concentrations change significantly;
- bottom layer, where the temperature, the water salinity and the oxygen concentrations become approximately constant.

In the surface layer, the calculated oxygen concentrations are in a perfect agreement with the measurements. Then, in the intermediate layer the model well predicts the trends in vertical distribution of oxygen. In the bottom layer, the calculated concentrations of oxygen are consistent with observations but do not match them very well. Generally, the vertical structure of oxygen is highly correlated with the measurements in each period of the year.

Correlation coefficient, R , normalised standard deviation, $\tilde{\sigma} = \sigma_m / \sigma_r$ (σ_r and σ_m are the standard deviations of the reference and the model field, respectively) and RMSD of simulated and measured oxygen concentrations are given in Table 2. The statistics are calculated on the basis of the available measurements of the full water column during the year

1998 at five stations and the corresponding simulated values. In addition to the statistics for the four studied stations, the statistics for the Landsort station, BY31, 440 m depth (see Fig. 1), is also presented to support the model validation. The measured oxygen concentrations of each observation have been interpolated on the computational grid of the water column and then R , $\tilde{\sigma}$, and RMSD are calculated (the same procedure has been done for the statistics presented in Table 3). It should be noted that the number of observations at each principle station is about 15 per year and the number of observation points in the water column related to the station depth is also similar for all stations. Therefore, we can consider the statistics of these stations as equally reliable. The model-data agreement is perfect for BY5, BY15 and BY31 and nearly perfect for the other two stations. The relatively low values of the RMSD in comparison to the variability of the data indicate a close match between predicted and observed concentrations. In summary, this information supports our conclusions that the model successfully reproduces the vertical water column variability of the oxygen.

5.2 Seasonal and interannual variability

5.2.1 Surface and intermediate layer

The model results are analysed at the previously identified three main water column layers for the period 1998-2003. Figure 5 shows the modelled time series of surface oxygen for stations BY0, BY1 and BY5 compared with the BED and FIMR data (see Fig. 2c for station BY15). The time interval between two subsequent major ticks in all time series plots is 2 months. At the surface, the modelled oxygen is in a near-perfect agreement with the observations. The observed increase of surface oxygen concentrations with decreasing surface temperature is well captured by the model. Some peaks of the oxygen concentrations are underestimated for BY0 (Fig. 5c) for the years 1999, 2002 and 2003. This is partially caused by the inflow of oxygenated surface water from the North Sea at this station. BY0 is placed in Kattegat, close to the North Sea, where the surface water salinity is affected by the irregular inflows and outflows of salty or brackish water, respectively. Despite this little misfit, the adequate accordance between simulations and data indicates that the parameterisation (1), (3) and (4) used to compute the surface oxygen flux is appropriate for the Baltic Sea and the time evolution of surface oxygen is mostly determined by the gas exchange at the surface.

The oxygen time series in the intermediate layer are shown in Figs. 6 and 7a-9a. In the intermediate layer the model matches very well the data, see the stations BY15 (50 m depth in

Fig. 6), BY5 (40 m depth in Fig. 7a) and BY1 (20 m depth in Fig. 8a). The discrepancy between calculated and observed concentrations of oxygen is higher at station BY0 (Fig. 9a). This is expected because the influence of horizontal advection is more pronounced at BY0 than at the other selected stations.

5.2.2 Bottom layer and inflow dynamics

The oxygen time series in the bottom layer are also shown in Figs. 6 and 7a-9a. However, the model performance in deep water layers, at the bottom, is not really satisfactory. The sediment oxygen demand is only partially taken into account in the model and therefore the simulated bottom oxygen is approximately constant in time at the deep stations BY15 and BY5. The modified model of Neumann et al. (2002) including a non-Redfield stoichiometry has not led to a significant improvement of the simulated near bottom oxygen at a station in the Central Gotland Sea (Kuznetsov et al., 2008). The introduction of a real sediment layer is still an ongoing development for this model. Contrary to the surface layer, the horizontal advection of oxygenated water is a very important component of the oxygen dynamics in the bottom layer. This can be clearly seen by the sudden increases in bottom oxygen in Figs. 6 and 7a, which are linked to the major inflow in January 2003.

Nevertheless, that the main hydrographic conditions of the Baltic Sea are characterised by permanent salinity stratification, these conditions are not the same for the different regions of the Baltic Sea. The bottom temperature is about constant except during inflow events for the stations of the Baltic Proper (see, for example, Fig. 7b) and varies seasonally at the BY1 (Fig. 8b) and BY0 (Fig. 9b). The variation of bottom salinity is also shown in Figs. 8c-9c, exhibiting very distinct features in the different regions. In the Kattegat area (BY0) occur frequent small variations (~ 1 PSU), in the Arkona basin (BY1) we find quasi seasonal large fluctuations (~ 10 PSU) and in the Bornholm Sea (BY5) there is a steady decrease interrupted by irregular inflow events.

When one compares the time series of bottom temperature and salinity with bottom oxygen at BY0, BY1 and BY5, several features of these time series can be underlined.

First, at the entrance area where station BY0 (small bottom salinity fluctuations) is placed, we find a strong negative correlation between observed temperature and oxygen fields of $R(T, O_2) = -0.82$. This seems to indicate that the bottom oxygen concentration at BY0 is

mainly determined by the inverse temperature dependent oxygen saturation and less by the sediment oxygen demand.

Second, the picture at BY1 is more complicated, as both temperature and salinity variations are influencing the bottom oxygen dynamics. For example, at the end of August 1999 there is a summer inflow of warm and salty water from the Belt Sea, at the same time oxygen is depleted and therefore it reaches a minimum (Fig. 8). A similar episode happens in July/August 2002. Contrary to these low oxygen summer inflows, the normal winter inflow of high salinity and low temperature is oxygen saturated (see the inflow in January 2003). As a consequence of these different inflow types, the correlation between observed temperature and oxygen fields in the bottom layer at BY1 is $R(T, O_2) = -0.57$.

Third, in the Baltic Proper, at BY5 the increase of oxygen usually corresponds to a sudden increase in salinity (Fig. 7). This relation is true also for bottom temperature and oxygen except for the winter inflow in 2003. The correlation between salinity and oxygen in the bottom layer seems to indicate that the increase of the near-bottom oxygen is due to infrequent pulses of North Sea inflow. The warmer inflows in October 1999 and December 2001 (Feistel et al., 2003) bring less oxygenated water, however they ventilate to some extent the bottom water at Bornholm station (Fig. 7). The decrease of oxygen during stagnation periods which is caused by the sediment oxygen demand is practically not captured by the model. It appears that at BY5 and BY15, the bottom oxygen flux is of higher importance for the oxygen concentration. Therefore, a better parameterisation of the oxygen depletion in the bottom layer might be essential.

In summary we can state that the seasonal variability of the bottom oxygen at stations BY0 and BY1 is only partially matched by the model, which can capture the variation to some extent, with a reduced range of amplitudes and with a phase shift of 1-2 months. The oxygen dynamics in the more central Baltic stations (BY5 and BY15) cannot be reproduced by a 1-D model. Although, the discrepancy between model and observation data is not only due to the omitted horizontal advection because the 3D circulation model used by Neumann et al. (2002) predicts also too high values of the near bottom oxygen at BY5 and BY15 (stations 213 and 271 in Fig. 13 of Neumann et al., 2002) for the period from 1983 until 1990. Unfortunately the simulation of the horizontal transport of their 3-D model is too diffusive (see the near bottom salinity in Fig. 5 of Neumann et al., 2002), so that likely in the simulations no inflowing oxygen rich water has arrived at the bottom of the Gotland Sea. In Neumann et al. (2005) the vertical resolution has been increased, which led to some improvement of the near

bottom oxygen concentrations. The calculated time series of near bottom oxygen is passing through the observation data but without showing any inflow dynamics. Evidently, the near bottom oxygen dynamics and near bed consumption are not well considered and further adjustments to the model are necessary. However, even the correct accounting of the sediment oxygen demand will not lead to improved simulations here, as we have to consider advection by applying a 3-D model or at least parameterize the effect of the inflow events on the oxygen concentrations for the 1-D runs.

5.2.3 Summary statistics for full water column

Summary statistics of the interannual model performance (Table 2) shows a high correlation between the observed and modelled values; the R and $\tilde{\sigma}$ are close to one, the RMSD are relatively small, although they are higher than those for the year 1998 (Table 1). The summary statistics are generally less favourable for BY0 and BY1 than for BY5 and BY15 with a lower correlation. Additionally, the modelled values of oxygen underestimate the measured ones ($\tilde{\sigma} = 0.71$ at BY1 and $\tilde{\sigma} = 0.65$ at BY0). The low values of the correlation coefficient at BY0 and BY1 are expectable because of the time shift in the bottom oxygen time series (Figs. 8 a and 9 a). This discrepancy is mainly due to the effect of inflow dynamics and oxygen sediment demand which are fairly considered in the model. Unfortunately, there is not enough observation data to check this assumption.

Thus, the statistics presented in Table 2 confirms the information obtained by the time-series plots (Figs. 6–9). It should be noted here that the agreement between modelled and observed oxygen concentrations will be a little better if we would exclude the year 2003 from the comparisons. This exclusion could be justified for our 1-D simulations because of the occurrence of the major inflow event in January 2003 (Feistel et al. 2003), which would require the consideration of horizontal oxygen transport.

5.2.4 Chlorophyll a simulation

Biological activity is another factor controlling oxygen concentrations. The interannual variability of simulated and observed average phytoplankton concentrations, shown as average chlorophyll a (Chla) is given in Fig. 10. The time series of calculated Chla concentrations and *in-situ* data of BED and FIMR correspond to the water column average values (from the surface to 20 m depth). Also presented in the figure are the monthly mean values taken from satellite images (Environmental Marine Information System (EMIS))

database, <http://emis.jrc.ec.europa.eu/>). The model predicts a spring bloom mostly composed of diatoms and flagellates in the beginning of March for BY5 (Fig. 10 a) and in the beginning of April for BY15 (Fig. 10 b). To some extent this result coincides with HELCOM (1996) report stating that the spring bloom of phytoplankton develops earlier at the western part of the Baltic Sea than in its eastern and northern parts. In these areas, a strong spring bloom develops in April/May, followed by a small summer bloom in July/August, and an autumn bloom in October/November. After mild winters, the spring bloom could appear earlier. Also, the regional differences in timing and strength of the spring bloom are related to the mixing depth (Wasmund et al., 1998) and the strength of the winter deep mixing (Janssen et al., 2004). There is a weak evidence of a summer bloom in the model results at BY5 (Fig. 10 a), however, it is not simulated for BY15 (Fig. 10 b) by the model. Typically, the autumn bloom is predicted to develop in September/October. The autumn peak is well phased and corresponds to all presented observation data. There is a reasonable agreement between the modelled and observed average Chla in 2003 at BY5, however, in all other years the model predicts lower bloom peaks than the observed ones at both stations BY5 and BY15. A part of the discrepancy between calculated concentrations of chlorophyll a and observed values could be explained by the simplified parameterisation used for chlorophyll in the model, which is a simple linear function of the N-content (Janssen et al., 2004). Still one has to keep in mind that comparing *in-situ* and model data involves many uncertainties, as the typical random pull of a bucket of water out of a patchy plankton bloom might lead to a drastic over- or underestimation of the real mean Chla concentrations in the measurement area. This could be overcome only by rather expensive measurement methods as for example taking about 100 random samples within the comparison region in order to establish statistical means and confidence intervals for the measurements. Additionally, as depicted in Fig. 10, there is not a good agreement between both measured data types (*in-situ* and satellite data). The satellite data are often missing the spring bloom peak, which might be related to cloud cover during that time. An interesting finding is that the model shows better succession in the phytoplankton content for the years when *in-situ* and satellite data match better. This might be an indication that in such a case of agreement the observed data are more representative of the real situation in the field. Despite the above mentioned limitations of the model, we can conclude that under the influence of atmospheric forcing and at different hydrographic characteristics the model reproduces the annual and interannual cycles of oxygen typical for the Baltic Sea.

6 Sensitivity analysis

Statistics, such as correlation coefficient, R , normalised standard deviation, $\tilde{\sigma}$, and the normalised “unbiased” root mean squared difference, \tilde{S} (normalised by σ_r) are used to compare the multiple model runs with the reference (observation) data. The difference between normalised RMSD and potential bias is denoted with \tilde{S} . The RMSD is a measure of the average magnitude of the difference, while \tilde{S} may be conceptualized as an overall measure of the agreement between the amplitude ($\tilde{\sigma}$) and phase (R) of two temporal patterns. For this reason, R , $\tilde{\sigma}$ and \tilde{S} are referred as “pattern statistics”. The three pattern statistics are related to one another by (Taylor, 2001)

$$\tilde{S} = \sqrt{1 + \tilde{\sigma}^2 - 2\tilde{\sigma}R}. \quad (5)$$

The normalised standard deviation and the correlation coefficient from the model to reference field comparisons may be displayed on a single Taylor diagram (for example, see Fig. 11). The Taylor diagram is a polar coordinate diagram with polar angle proportional to $\arccos(R)$ and radial distance from the origin proportional to $\tilde{\sigma}$. Therefore the reference field point has the polar coordinates (1.0, 0). The model to reference comparison points are then assessed by how close they fall to the reference point. This distance is equal to \tilde{S} . The relationship (5) makes the Taylor diagram useful because the individual contribution of misfits of amplitude may be compared to misfits in phase to distinguish how they contribute to the normalised unbiased RMSD. The same as for statistics presented in Table 2, all calculations have been done on the basis of all the available measurements of the full water column during the period 1998-2003 and the corresponding model results. It is important to note that the model and reference fields are not log-transformed or averaged in all presented comparisons.

6.1 Effect of vertical turbulent exchange

The results of 11 separate model runs with different values of k_{\min} are shown in Fig. 11. It is a Taylor diagram of the sensitivity of the model to the vertical turbulent exchange. The diagram shows the model to reference statistics for the oxygen, phosphorus, ammonium, nitrate and chlorophyll a fields during the period 1998-2003 at BY5. The parameter investigated here is

the minimum turbulent kinetic energy, k_{\min} , which is used in the turbulence model as a parameterisation to account for unresolved mixing processes as e.g. internal waves (Burchard et al., 2006). The colour bar represents 10 different values of $k_{\min} \cdot 10^7$ in the interval [5; 30]. Generally, the model performance is the best for oxygen (the highest R values and the smallest \tilde{S} values). Limiting nutrients have an intermediate goodness of fit (R values ranging from 0.4 to 0.8 and \tilde{S} values from 0.65 to 1) and chlorophyll a has the highest misfit with the observed values. The spread of comparison points in Fig. 11 demonstrates that k_{\min} is an important parameter for predicting all the presented state variables. Since our interest is mainly related to the oxygen dynamics, we will discuss in detail the sensitivity of oxygen to changes in the vertical turbulent mixing. Figure 11 clearly indicates that the model overestimates the interannual cycle at low k_{\min} ($< 7 \cdot 10^{-7} [m^2/s^2]$) and underestimates it at high k_{\min} ($> 15 \cdot 10^{-7} [m^2/s^2]$). The value of $\tilde{\sigma}$ changes rapidly with increasing k_{\min} , while the value of R does not. In other words, the vertical turbulent mixing has a higher influence on the amplitude rather than on the phase of the simulated oxygen field. Both minimum of the total RMSD (indicated by “ \diamond ”) and minimum of the unbiased RMSD are found for $k_{\min} = 1 \cdot 10^{-6} [m^2/s^2]$. Thus, the bias between modelled and reference fields has also a minimum at this point. We have found the best fit between the model and reference oxygen fields at BY15 for $k_{\min} = 8 \cdot 10^{-7} [m^2/s^2]$, at BY1 for $k_{\min} = 25 \cdot 10^{-7} [m^2/s^2]$, at BY0 for $k_{\min} = 80 \cdot 10^{-7} [m^2/s^2]$, while at BY31 for $k_{\min} = 5 \cdot 10^{-7} [m^2/s^2]$. It appears that k_{\min} is an important model parameter and one must decide carefully how to parameterise it when one couples the GOTM-BIO_IOW model with a 3-D circulation model of the Baltic Sea.

There is a trend of decreasing the optimal k_{\min} (80; 25; 10; 8; 5) $\cdot 10^{-7} [m^2/s^2]$ with the distance from the entrance of the Baltic Sea, which might reflect the decrease in the effective vertical exchange in the Baltic. The strength of the density stratification expressed as the observed mean vertical density difference, $\rho_t [kg/m^3]$ for the period 1998-2003, shows a similar spatial pattern: 11.56 at BY0; 8.17 at BY1; 8.63 at BY5; 6.4 at BY15 and 6.41 at BY31.

6.2 Effect of relaxation to temperature and salinity profiles

As it has been mentioned in Sect. 3, the model is forced by prescribed depth profiles of temperature (T) and salinity (S) among the other forcing. The relaxation to the T and S profiles is necessary for 1-D simulations in an environment where lateral processes cannot be neglected (Reissmann et al., 2009). It is found that the model performance depends on the salinity relaxation time scale rather than that of temperature. All model results presented above have been calculated by applying the observation data of BED for relaxation. The best fit for oxygen is found for a relaxation time of 5 days. In order to study how the variability of T and S tracer concentrations used for relaxation will affect the oxygen dynamics in the different stations, we have applied also profiles from 3-D model simulations. In Fig. 12 are given the normalised pattern statistics of T , S and oxygen (O). For each station two separate model runs are made using different profiles for temperature/salinity (T/S) relaxation. The small letters refer to the results obtained by using observed profiles of BED for relaxation and the capital letters refer to the 3-D model relaxation. The pattern statistics of T , S and O are normalised by the standard deviation of the corresponding observation field. The colour of all letters is altered for each station. Figure 12 indicates that the statistical properties of the 3-D model fields are of good (T) or reasonable (S) quality at all stations. The normalised standard deviation of the T field is in the interval $[0.89; 1.08]$ and $R \geq 0.94$. The salinity concentrations are not so well simulated when using the 3-D profiles. Especially, the amplitude of the model S field is significantly lower than that of observed field ($\tilde{\sigma} = 0.45$ of S at BY15), while it is well phased for all stations ($R \geq 0.88$).

From the Taylor diagram shown in Fig. 12 it can be seen that the forcing with BED data gives slightly better results. The close coincidence of the oxygen comparison symbols for BY0 and BY1 (yellow and green) points to the low sensitivity of the oxygen dynamics at these stations to the prescribed salinity field. The influence of the T/S forcing data is more pronounced for the other two stations and in particular for BY5 where $\tilde{\sigma} = 0.8$ and $R = 0.95$ in the case of the 3-D model profiles, however the agreement with observation data is rather better in the case of using the BED profiles (see Table 3). Despite the underestimation of salinity, the good results for oxygen demonstrate that it is possible to utilise 3-D model data for T/S relaxation in all cases when observation data is scarce or absent.

6.3 Effect of atmospheric forcing

In order to investigate the model sensitivity to variations of the atmospheric forcing, we present results from five different cases and compare them with the observation data. The normalised pattern statistics of oxygen have been calculated for the period 1998-2003 after varying the wind speed values in the ERA-40 re-analysis data. Namely, the wind speed has been rescaled by a factor of 0.5, 0.8, 1.0, 1.2, and 1.5 (plotted with different colours in Fig.13). The value of k_{\min} is fixed to its best fit value which is different for each particular station (see the values of k_{\min} already reported in Sect. 6.1). The close grouping of the comparison points for BY15 (circles) indicates that the oxygen dynamics at this deep station is not sensitive to a possible uncertainty in the forcing data. We get significant changes in the modelled oxygen for all other stations. Particularly, when the wind speed is scaled down the comparison points are farther away from the reference ones than when it is scaled up. In summary, one can conclude that an increase of wind speed by a factor of 1.2 has led to a general improvement in the model performance. For the scaling factor of 1.5 the correlation is slightly improved for BY0 and BY1, even though the results for $\tilde{\sigma}$ and \tilde{S} are worse for BY5. Another possible inference drawn from Fig. 13 could be that the wind speed magnitude of the ERA-40-reanalysis could be underestimated.

6.4 Effect of limiting nutrients

In the model, the nutrient load is taken into account via initial concentrations and surface fluxes of nitrate, phosphate and ammonium. For the 1-D model considered here, the nutrient fluxes at the air-sea surface have to be adjusted in order to parameterise lateral nutrient fluxes. A Taylor diagram is drawn in Fig. 14 for testing the model sensitivity to limiting nutrients, showing the model to reference statistics for oxygen (red) and chlorophyll a (green) at BY5. The results of 150 separate model runs are shown on the diagram and the corresponding intervals from which the initial concentrations and the surface fluxes of nutrients are randomly chosen are given in Table 3. The surface fluxes of nutrients are assumed as constants during one model run. The average values (for the upper 20 m) of chlorophyll a are used for comparisons. It appears that both oxygen and chlorophyll a are weakly sensitive to the variation in the concentrations of nutrients. Moreover, only the amplitude of the model oxygen field is sensitive, while the phase remains approximately unchanged ($R \cong 0.95$). The low sensitivity of the oxygen and chlorophyll a fields to a relatively big variation in the values

of the nutrient surface fluxes could be explained with the simple parameterisation of the fluxes, which is used here, – as a constant. Typically, the surface water concentrations of nutrients in the Baltic Sea are very low in summer and high in winter. The comparison points with the minimum RMSD values are indicated by a black diamond (“◊”) in Fig. 14. It worth to note, that at these points the unbiased RMSDs have also a minimum. The initial concentrations and surface fluxes of nutrients for which we have found the best fits for oxygen and chlorophyll a are given in Table 3.

7 Summary and Conclusions

In the present work we have examined the influence of some important physical and geochemical factors on the oxygen concentrations at several regions of the Baltic Sea. For this purpose we used the GOTM-BIO_IOW model. The model has been forced with meteorological data for a six year period. Modifications in the parameterisation of the air-sea oxygen fluxes have led to a significant improvement of the model results in the surface and intermediate water levels. A model validation has been done by evaluating the agreement between predicted values of oxygen and observation data from the BED and FIMR data bases. The correlation with observation data is good and consistent for all stations and with low values of the RMSD (Tables 1 and 2). Specifically the oxygen dynamics of the surface mixed layer is simulated in close agreement with the observations. The fact that the oxygen dynamics at the surface can be accurately simulated by a 1-D model has been already shown by Vichy et al. (2004) for the BY5 during the stagnation period 1979-1990 and by Kuznetsov et al. (2008) for the Central Baltic Deep during 1978-1993. However, it comes certainly at a surprise that even the very dynamic transitional stations BY0 and BY1 are very well simulated by the 1-D model, which is ignoring completely the advection of oxygen. And this remains true even in the case when a major inflow event appears like this in 2003. Therefore, it can be concluded that in the surface layer the dynamics of the mixed layer and the oxygen exchange with the atmosphere are the controlling factors of near surface oxygen development. As it has been shown, these physical factors also clearly dominate the biological production and respiration of oxygen at the surface layer.

The largest mismatch with observations is found in simulating the bottom water oxygen dynamics. This is of course expected, as the bottom oxygen concentrations in the Baltic Sea are not only determined by the local sediment oxygen demand, but largely influenced by

inflowing oxygenated water from the North Sea. As we have not taken into account the horizontal advection of oxygen in the 1-D model, we could not simulate the increase of bottom oxygen during inflow events. Nevertheless, it is obvious that the oxygen consumption at the sediment interface demands for an improved parameterisation. However, one has to keep in mind that when incorporating a better sediment oxygen demand parameterisation in a 1-D model, the results of the simulation could become worse because of the fact that an eventual higher consumption will not be counterbalanced by oxygen transport. The statistical properties of the modelled nutrient and phytoplankton concentrations are also reasonable. This demonstrates the good capability of the model to predict the oxygen dynamics at all selected stations.

The results emphasise the importance of the principal hydrographic situation, the accuracy of the hydrographic characteristics, the variability of the vertical turbulent exchange and atmospheric forcing, the parameterisation of the air-sea oxygen exchange and quantity of the nutrient supplies. It is found that these mechanisms play an important role in the oxygen dynamics of the water column of the Baltic Sea. The model results point out the significant differences between the oxygen cycles in the different regions of the Baltic Sea. For the selected six year simulation period the concentrations of deepwater oxygen change seasonally at Fladen and Arkona and have almost no seasonal variability at the two stations in the Baltic Proper. Sensitivity analysis has been performed in order to examine the influence of turbulent mixing, hydrographic forcing (salinity and temperature profiles used for relaxation), atmospheric forcing (wind speed), and nutrient loads. The normalised standard deviation, the correlation coefficient and the normalised unbiased RMSD from each model to reference field comparison are displayed as Taylor diagrams. It is found that the natural physical factors, like the magnitude of the vertical turbulent mixing, wind speed, the variation in temperature and salinity are the major factors controlling the oxygen dynamics in the Baltic Sea. The influence of limiting nutrients is less pronounced, at least under the nutrient flux parameterisation assumed in the model.

The interesting fact that the minimum kinetic energy used in the turbulence model giving the best fit of simulations to observations is decreasing with the distance from the entrance of the Baltic Sea, namely, $k_{\min} = (80; 25; 10; 8; 5) \cdot 10^{-7} [m^2 / s^2]$, could be a hint to unresolved mixing due to e.g. breaking internal waves as the strength of the density stratification is decreasing in a similar way. Further this clearly underlines the fact that the use of a spatial

and temporal constant k_{\min} in 3-D applications is inappropriate, an improved parameterisation is urgently needed.

Acknowledgement:

We are grateful to the Baltic Nest Institute, Stockholm University and the Finnish Institute of Marine Research for making available the hydrographic and chemical data through the Baltic Environmental Database.

Special thanks go to the GOTM developers for providing and maintaining the model. The critical comments of an anonymous referee and suggestions by Hans Burchard and Dimitar Marinov helped us to improve the manuscript.

References

- Axell, L. B.: On the variability of Baltic Sea deep-water mixing, *J. Geophys. Res.*, 103, 21,667-21,682, 1998.
- Baretta, J.W., Ebenhöf, W., and Ruardij, P.: An overview over the European Regional Sea Ecosystem Model, a complex marine ecosystem model. *Neth. J. Sea Res.* 33 (3/4), 233-246, 1995.
- Blackford, J. C, Allen J. I. and Gilbert F. J.: Ecosystem dynamics at six contrasting sites: a generic modelling study, *J. Marine Syst.* 52, 191-215, 2004.
- Bonsdorff, E., Rönnerberg, C., and Aarnio, R.: Some ecological properties in relation to eutrophication in the Baltic Sea, *Hydrobiologia* 475-476, 371-377, 2001.
- Feistel R., Nausch G., Matthäus W., and Hagen E.: Temporal and spatial evolution of the Baltic deep water renewal in spring 2003, *Oceanologia*, 45,623-642, 2003.
- Feistel, R., Nausch, G., and Hagen, E.: Unusual inflow activity 2002/3 and varying deep-water properties, *Oceanologia* 48 (S), 21-35, 2006.
- Burchard, H., Bolding, K., Kühn, W., Meister, A., Neumann, T., and Umlauf, L.: Description of a flexible and extendable physical--biogeochemical model system for the water column, *Journal of Marine Systems*, 61, 180-211, 2006.

- Feistel, R., Nausch, G., and Hagen, E.: The Baltic inflow of autumn 2001, *Meereswiss. Ber.*, 54, 55–68, 2003.
- Feistel, R., Nausch, G., Matthäus, W., and Hagen, E.: Temporal and spatial evolution of the Baltic deep water renewal in spring 2003, *Oceanologia*, 45 (4), 623–642, 2003.
- HELCOM: Third periodic assessment of the state of the marine environment of the Baltic Sea, 1989–1993, Background document, Baltic Sea Environ. Proceeding No. 64 B, Helsinki Commission, Helsinki, Finland, 1996.
- HELCOM: The Baltic marine environment 1999-200, Baltic Sea Environ. Proceeding No. 87, Helsinki Commission, Helsinki, Finland, 2003.
- HELCOM: Activities 2006 overview, Baltic Sea Environ. Proceeding No. 112, Helsinki Commission, Helsinki, Finland, 2007.
- IOW: Cruise Report of r/v "Alexander v. Humboldt", Cruise No. 44 / 03 / 07, Baltic Sea Research Institute, Warnemünde, Germany, 2003.
- Jakobsen, F.: The major inflow to the Baltic Sea during January 1993, *J. Mar. Syst.*, 6, 227–240, 1995.
- Janssen, F., Neumann, T., and Schmidt, M.: Inter-annual variability in cyanobacteria blooms in the Baltic Sea controlled by wintertime hydrographic conditions, *Mar. Ecol. Prog. Ser.*, 275, 59-68, 2004.
- Kuznetsov, I., Neumann, T., and Burchard, H.: Model study on the ecosystem impact of a variable C:N:P ratio for cyanobacteria in the Baltic Proper, *Ecological Modelling*, 219, 107-114, 2008.
- Kühn, W., and Radach, G.: A one-dimensional physical-biological model study of the pelagic nitrogen cycling during the spring bloom in the northern North Sea (FLEX '76), *Journal of Marine Research*, 55, 687-734, 1997.
- Laamanen, M., Fleming, V., and Olsonen, R.: Water transparency in the Baltic Sea between 1903 and 2004. FIMR, Indicators 2004, State of the Baltic Sea, HELCOM (www.helcom.fi/), 2004.
- Lass, H. U., and Mohrholz, V.: On dynamics and mixing of inflowing saltwater in the Arkona Sea, *J. Geophys. Res.*, 108(C2), 3042, doi:10.1029/2002JC001465, 2003.

Liss, P.S., and Merlivat, L.: Air-sea exchange rates: introduction and synthesis. In: Buat-Menard, P. (Ed). The role of air-sea exchange in geochemical cycling. Reidel, Dordrecht, 163-170, 1986.

Matthäus, W., and Nausch, G.: Hydrographic-hydrochemical variability in the Baltic Sea during the 1990s in relation to changes during the 20th century, ICES Mar. Sci. Symp., 219, 132–143, 2003.

Mohrholz, V., Dutz, J., and Kraus, G.: The impact of exceptionally warm summer inflow events on the environmental conditions in the Bornholm Basin, J. Mar. Sys., 60, 285–301, doi:10.1016/j.jmarsys.2005.10.002, 2006.

Nausch, G., Matthäus, W., and Feistel, R.: Hydrographic and hydrochemical conditions in the Gotland Deep area between 1992 and 2003. Oceanologia 45, 557–569, 2003.

Neumann, T.: Towards a 3D-ecosystem model of the Baltic Sea, J. Mar. Sys., 25, 405–419, 2000.

Neumann, T., Fennel, W., and Kremp, C.: Experimental simulations with an ecosystem model of the Baltic Sea: a nutrient load reduction experiment, Glob. Biogeochem. Cycles, 16, 450, doi:10.1029/2001GB001, 2002.

Neumann, T., and Schernewski, G.: An ecological model evaluation of two nutrient abatement strategies for the Baltic Sea, J. Mar. Sys., 56, 195–206, 2005.

Omstedt, A., and Axell, L.: Modeling the seasonal, interannual and long-term variations of salinity and temperature in the Baltic proper, Tellus, 50A, 637-652, 1998.

Omstedt, A., Elken, J., Lehmann, A., and Picchura, J.: Knowledge of the Baltic Sea physics gained during the BALTEX and related programmes, Progress in Oceanography, 63, 1-28, 2004.

Reissmann, J.: On the representation of regional characteristics by hydrographic measurements at central stations in four deep basins of the Baltic Sea, Ocean Sci., 2, 71–86, www.ocean-sci.net/2/71/2006/, 2006.

Reissmann, J., Burchard, H., Feistel, R., Hagen, E., Lass, H.U., Mohrholz, V., Nausch, G., Umlauf, L., and Wicczorek, G.: State-of-the-art review on vertical mixing in the Baltic Sea and consequences for eutrophication, Progr. Oceanogr., 82, 47-80, 2009.

Sellschopp, J., Arneborg, L., Knoll, M., Fiekas, V., Gerdes, F., Burchard, H., Lass, U., Mohrholz, V, and Umlauf, L.: Direct observations of a medium-intensity inflow into the Baltic Sea, *Continental Shelf Research* , 2393-2414, [doi:10.1016/j.csr.2006.07.004](https://doi.org/10.1016/j.csr.2006.07.004) , 2006.

Stigebrandt, A.: Computations of oxygen fluxes through the sea surface and the net production of organic matter with application to the Baltic and adjacent seas, *Limnol. Oceanogr.*, 36, 444-454, 1991.

Stips, A., Bolding, K., Burchard, H., Djavidnia, S., and Peneva, E.: Realistic multiannual simulations of the coupled North Sea and Baltic Sea system using the GETM model, European Commission, EUR 21503 EN, 2005.

Vichi, M., Ruardij, P., and Baretta, J.W.: Link or sink: a modelling interpretation of the open Baltic biogeochemistry, *Biogeosciences*, 1, 79–100, 2004.

Wasmund, N., Nausch, G., and Matthäus, W.: Phytoplankton spring blooms in the southern Baltic Sea—spatio-temporal development and long-term trends, *Journal of Plankton research*, 20, 1099-1 117, 1998.

Weiss, R. F.: The solubility of nitrogen, oxygen and argon in water and seawater. *Deep-Sea Res.*, 17, 721-735, 1970.

Table 1. Impact of the parameterisation of the air-sea oxygen exchange and primary production on the surface oxygen concentrations.

Cases	Parameterisation of air-sea oxygen exchange	Mean absolute error [mlO_2 / l]	Correlation coefficient, R	RMSD [mlO_2 / l]
(I)	Eqs. (1) - (2), $V = 5 [m / d]$.	0.401	0.880	0.995
(II)	Eqs. (1) - (2), $V = 5 [m / d]$, Weiss formula for O_{sat} .	0.186	0.892	0.519
(III)	Eqs. (1) – (4).	0.150	0.957	0.610
(IV)	Eq. (1), Weiss formula for O_{sat} and Eqs. (3) – (4) for V .	0.00046	0.964	0.283
(V)	Without phytoplankton growth and grazing; oxygen exchange is calculated as in the case IV.	0.219	0.939	0.435

Table 2. Correlation coefficient, R , normalised standard deviation, $\tilde{\sigma}$, and root mean square difference, RMSD [mlO_2/l], of the simulated and measured oxygen concentrations in the full water column for n days of the year 1998.

Year 1998	Fladen	Arkona	Bornholm	Gotland	Landsort
n	16	15	14	15	32
R	0.83	0.83	0.97	0.98	0.99
$\tilde{\sigma}$	0.80	0.94	1.0	0.91	0.94
RMSD	0.61	0.69	0.67	0.95	0.69

Table 3. Correlation coefficient, R , normalised standard deviation, $\tilde{\sigma}$, and root mean square difference, RMSD [mlO_2/l], of the simulated and measured oxygen concentrations in the full water column for n days during the period 1998-2003.

1998-2003	Fladen	Arkona	Bornholm	Gotland
n	96	80	78	77
R	0.79	0.80	0.97	0.96
$\tilde{\sigma}$	0.65	0.71	1.00	0.79
RMSD	0.79	0.88	0.71	1.78

Table 4. Ranges of initial concentrations and surface fluxes of limiting nutrients used in the sensitive analysis. Corresponding values, for which the minimum of the RMSD has been found.

	Phosphorus	Nitrate	Ammonium
Range of initial concentrations [$mmol N / m^3$]	0.5 - 0.7	4 - 9	0.1 - 0.5
Range of surface fluxes [$mmol N / m^2 d$]	0.03 - 0.1	0.5 - 1	0.2 - 0.8
Initial concentrations [$mmol N / m^3$]			
with the minimum RMSD for oxygen	0.6	8.	0.4
with the minimum RMSD for chlorophyll	0.6	7.	0.3
Surface fluxes [$mmol N / m^2 d$]			
with the minimum RMSD for oxygen	0.06	0.7	0.4
with the minimum RMSD for chlorophyll	0.05	0.7	0.7

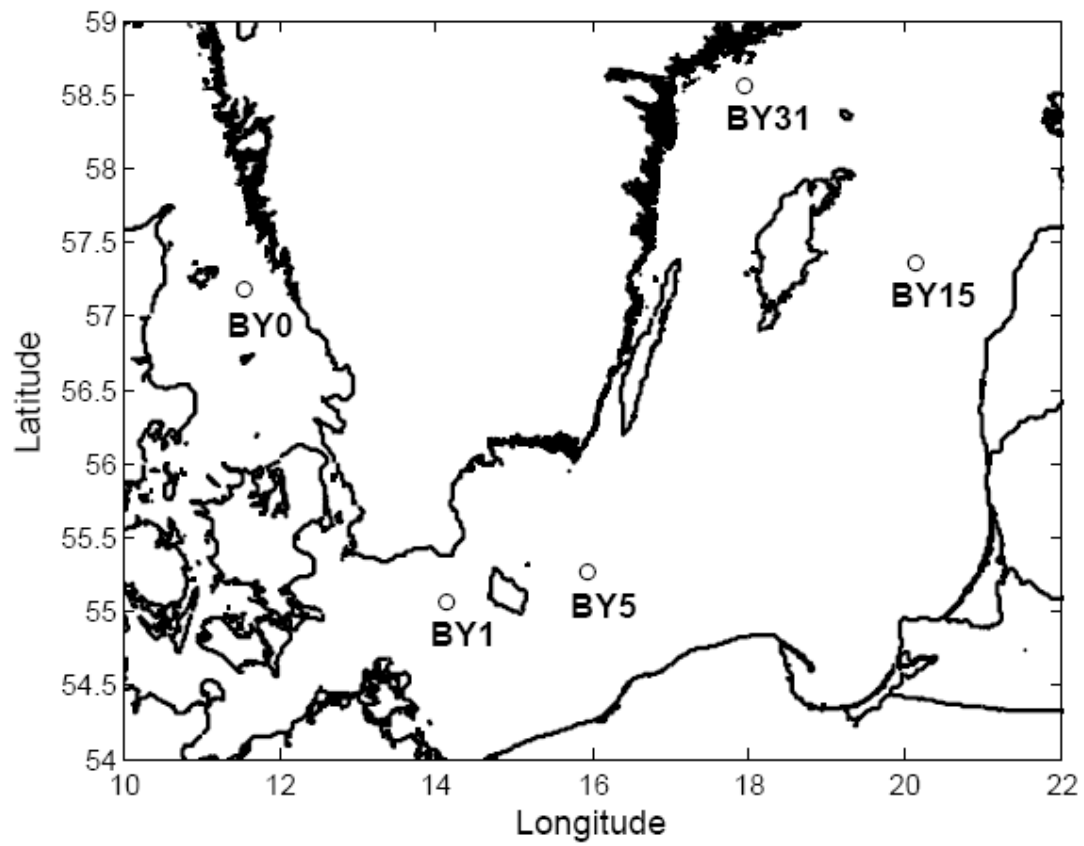


Figure 1. Map of the Baltic Sea showing the sampling stations: Fladen (BY0), Arkona (BY1), Bornholm (BY5), Gotland (BY15) and Landsort (BY31).

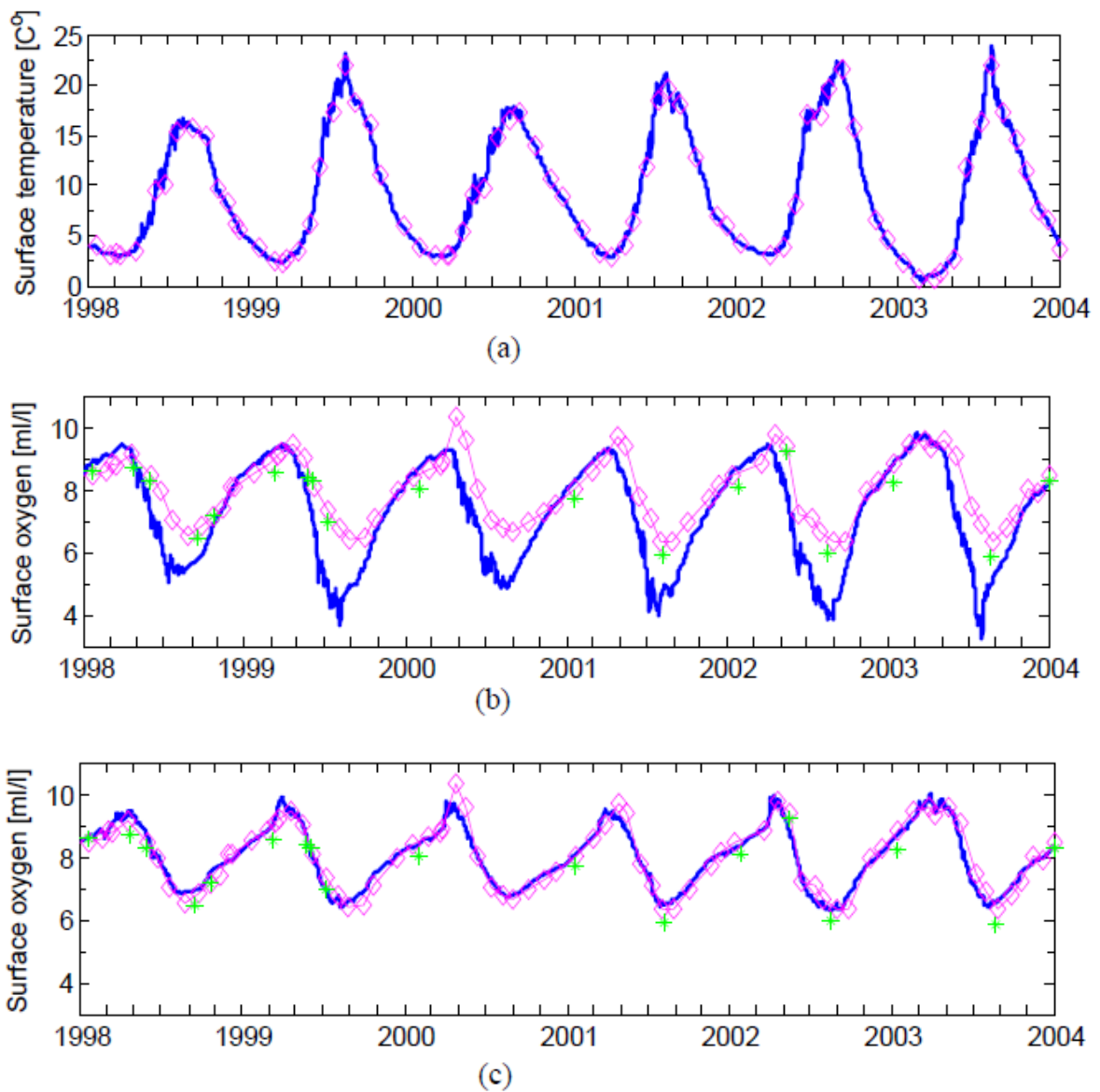


Figure 2. Modelled (thick solid line) and observed (symbols) values at BY15 of (a) - surface temperature, (b) surface oxygen calculated by using GOTM-BIO_IOW and (c) surface oxygen calculated from Eqs. (1), (3) and (4), and the formula of Weiss (1970) (case IV). Diamonds represent BED data, while asterisks represent FIMR data.

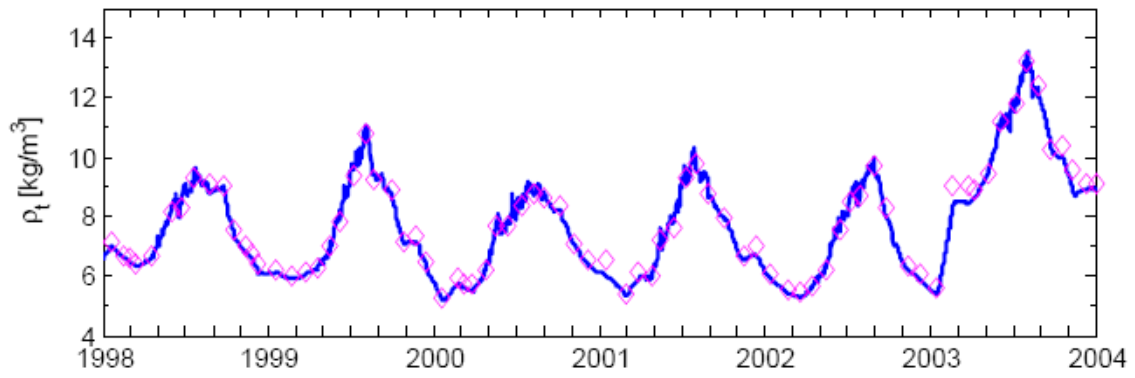


Figure 3. Modelled (solid line) and observed (symbols) density difference at BY5.

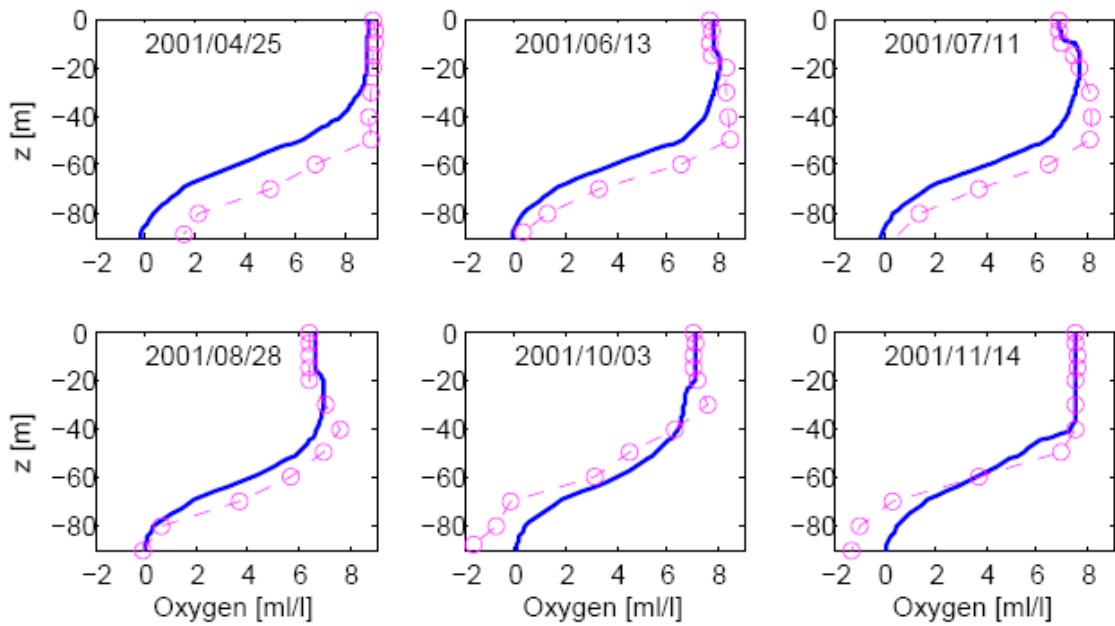


Figure 4. Vertical oxygen profiles at BY5 in some selected days of 2001. Calculated results are presented with a solid line, while circles connected with a dashed line show the observation data of BED.

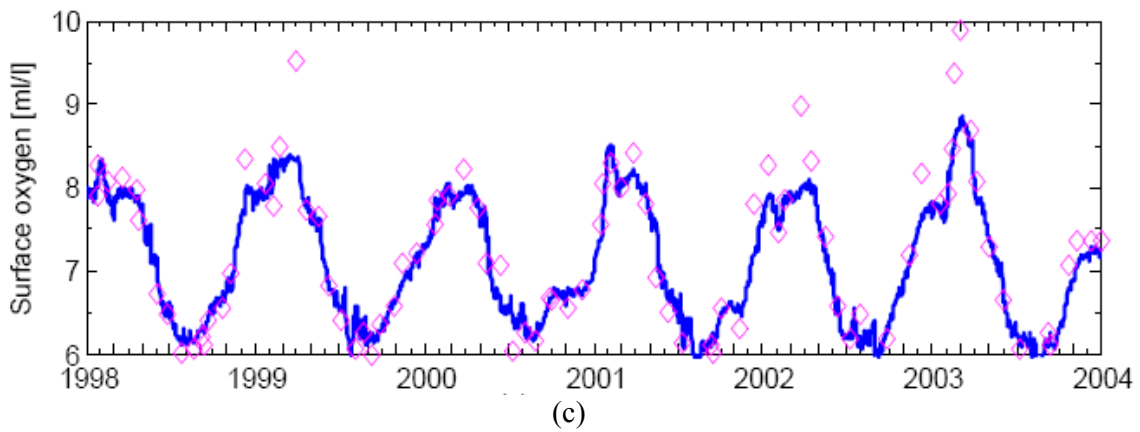
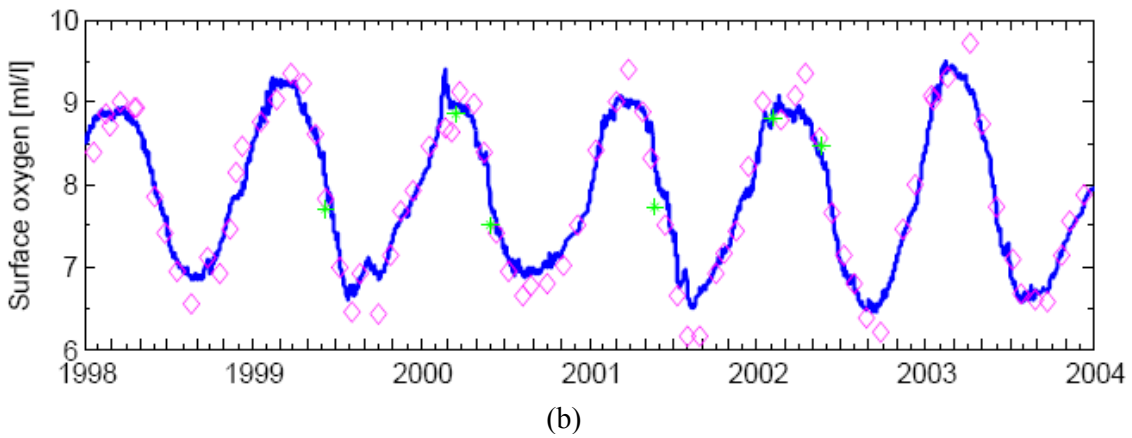
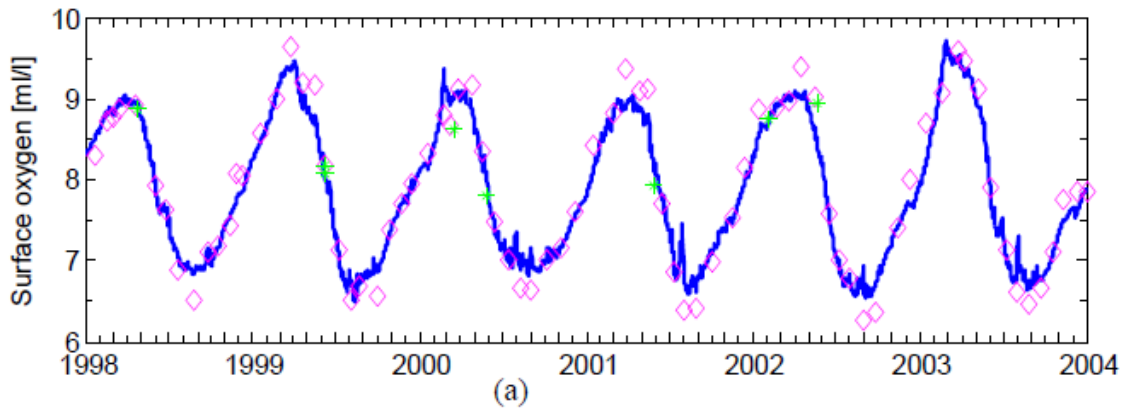


Figure 5. Time series of surface oxygen for the period 1998-2003. Calculated results are presented with a thick solid line, FIMR data with asterisks, and BED data with diamonds. (a) at BY5; (b) at BY1; (c) at BY0.

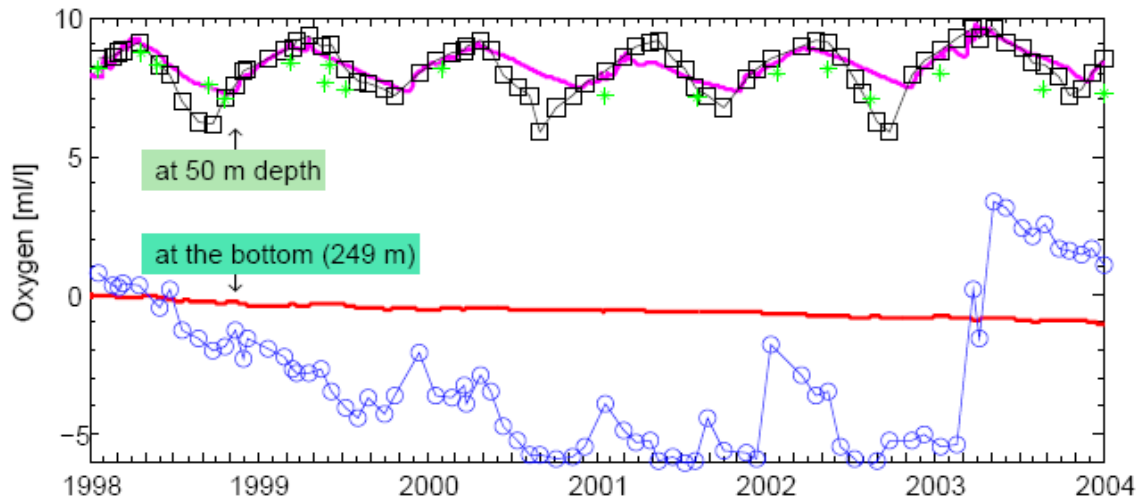
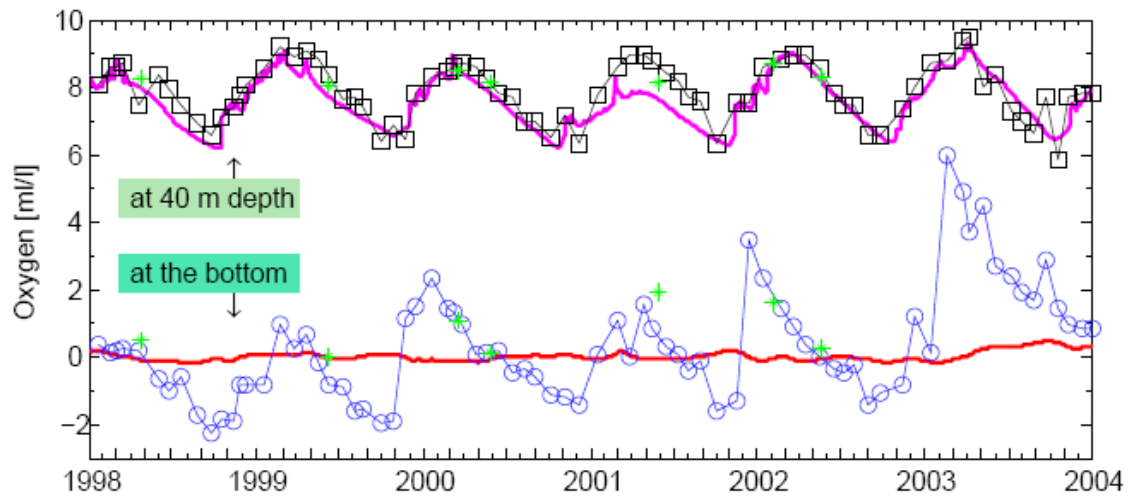
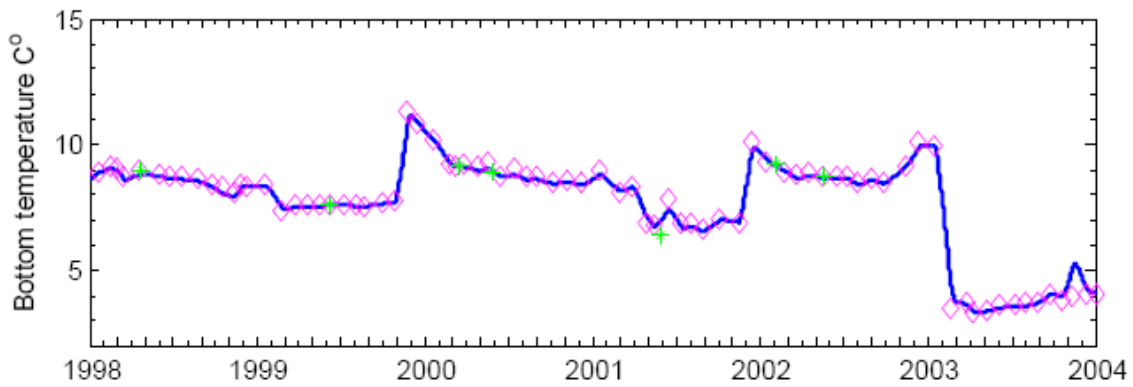


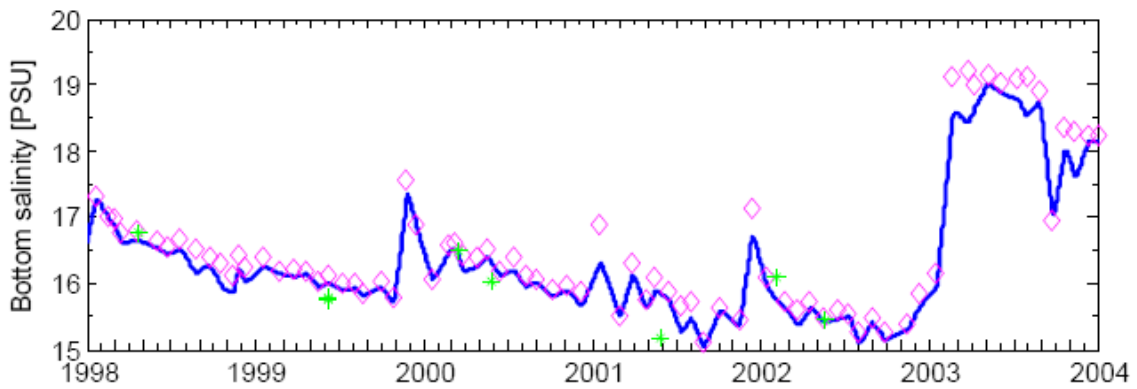
Figure 6. Oxygen time series at BY15 for the period 1998-2003. Calculated results are presented with a thick solid line, FIMR data with asterisks, and BED data with squares and circles. Time series are plotted at 50 m depth (magenta line and black squares) and at the bottom (red line and blue circles).



(a)

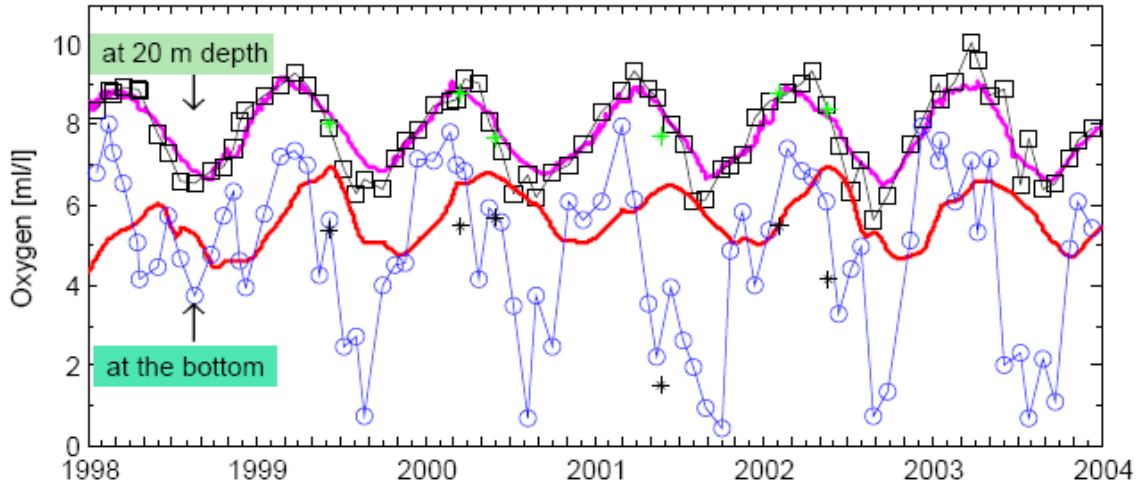


(b)

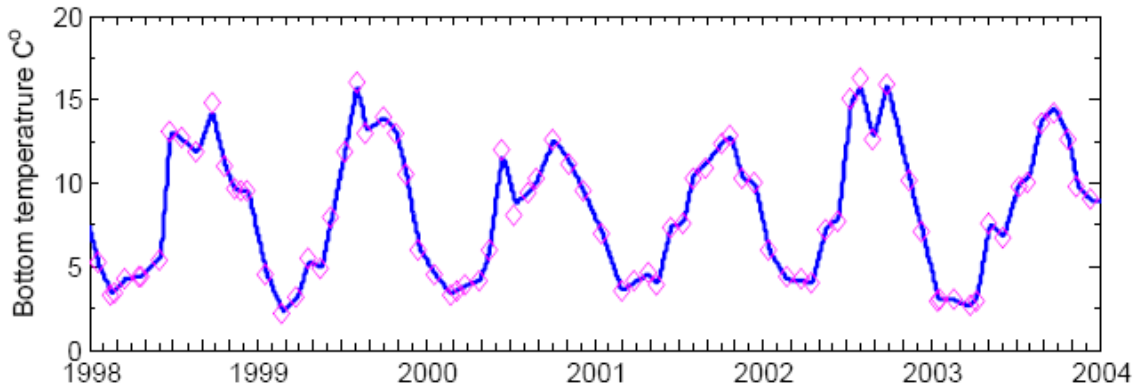


(c)

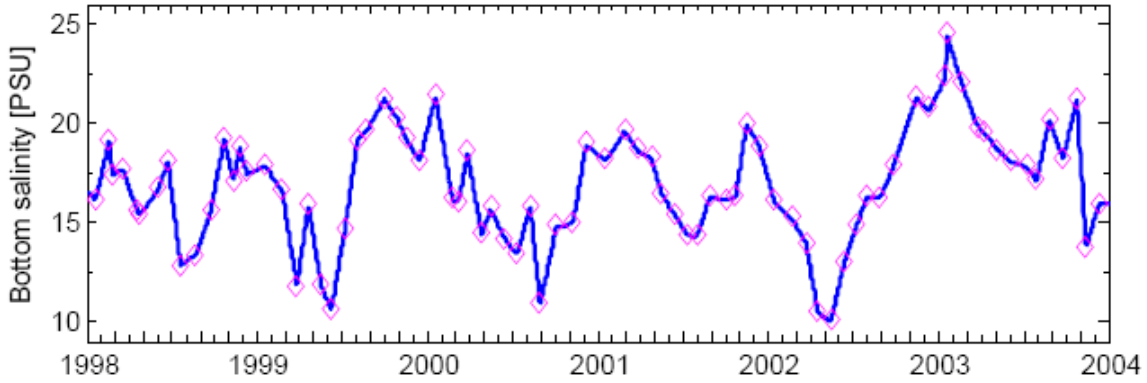
Figure 7. Time series at BY5 for the period 1998-2003. Calculated results are presented with a thick solid line and observation data of BED and FIMR with symbols (see capture of Fig. 6 for more details). (a) – oxygen at 40 m depth and at the bottom; (b) – bottom temperature (c) - bottom salinity.



(a)



(b)



(c)

Figure 8. Time series at BY1 for the period 1998-2003. Calculated results are presented with a thick solid line and observation data of BED and FIMR with symbols (see capture of Fig. 6 for more details). (a) – oxygen at 20 m depth and at the bottom; (b) – bottom temperature (c) - bottom salinity.

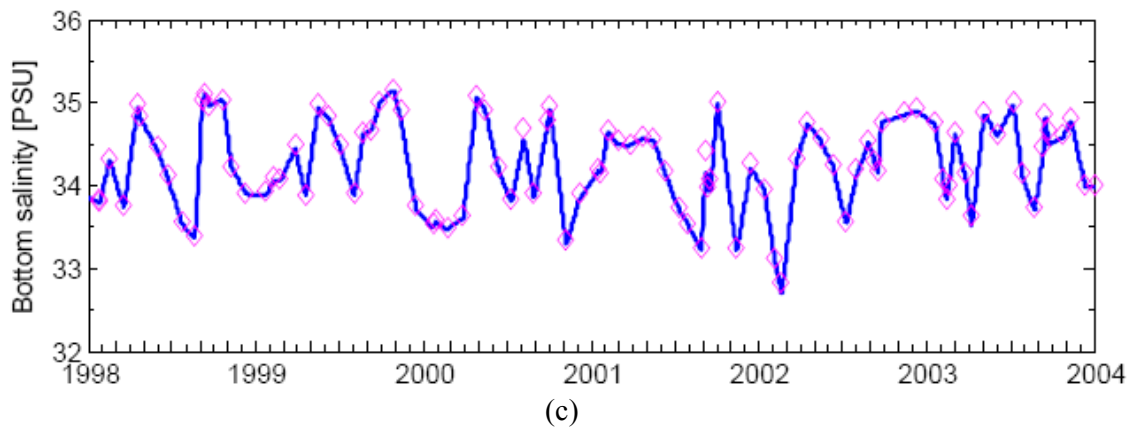
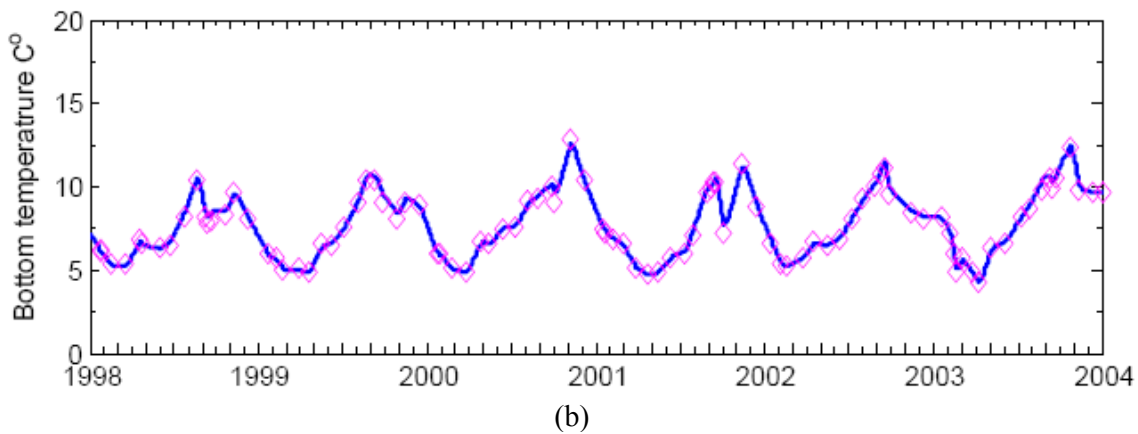
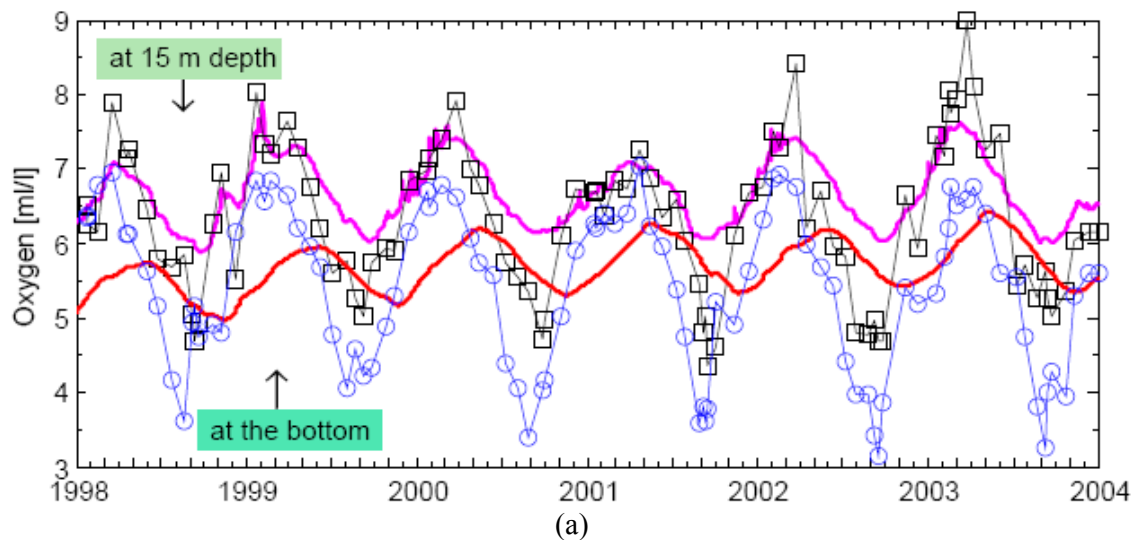


Figure 9. Time series at BY0 for the period 1998-2003. Calculated results are presented with a thick solid line and observation data of BED with symbols. (a) – oxygen at 15 m depth and at the bottom; (b) – bottom temperature (c) - bottom salinity.

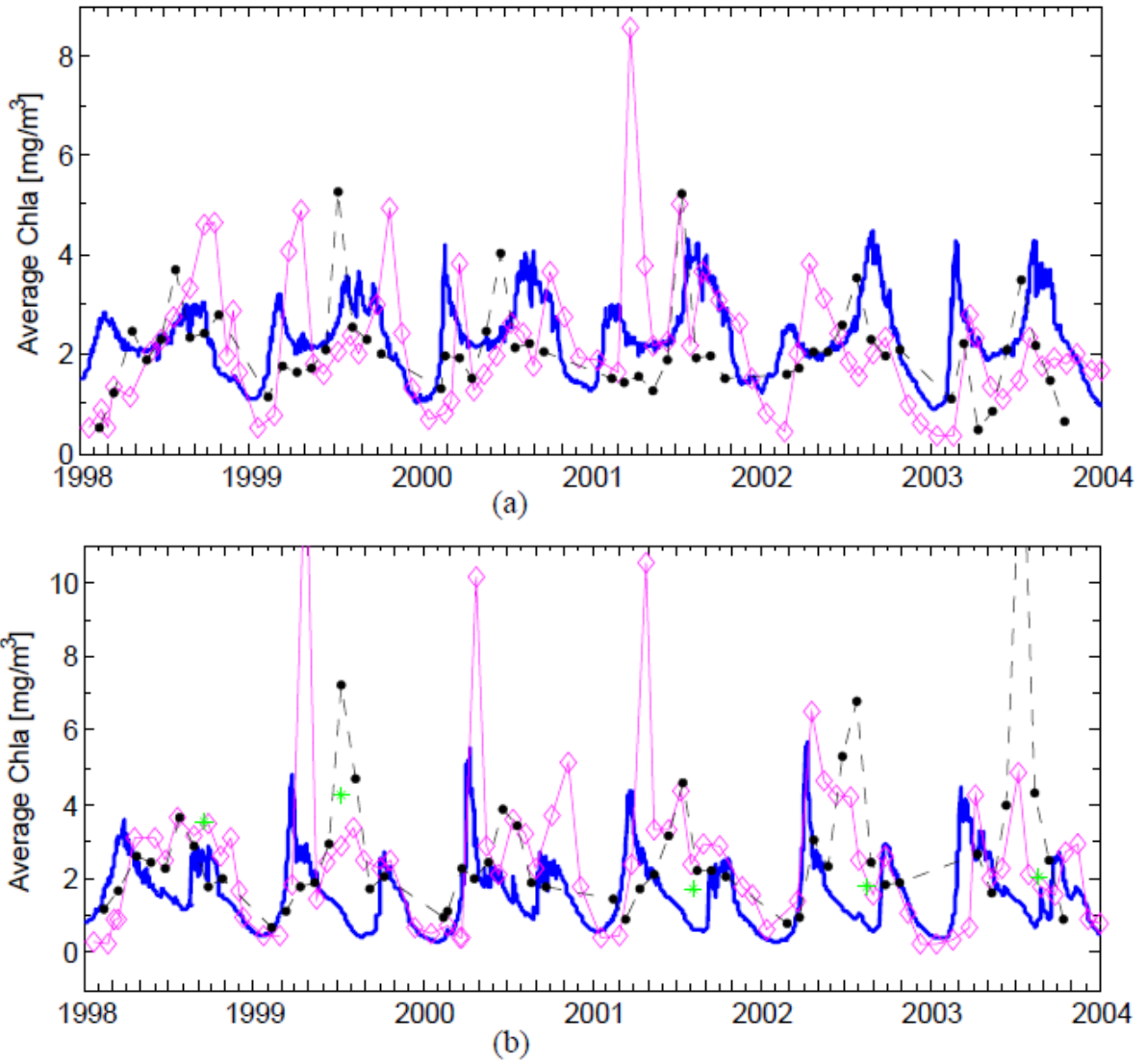


Figure 10. Modelled (thick solid line) and *in-situ* data (denoted with blank diamonds and asterisks) of average Chla [mg/m³] at: (a) - BY5, (b) - BY15. Data from satellite images (EMIS database) is presented with filled circles connected with a dash line.

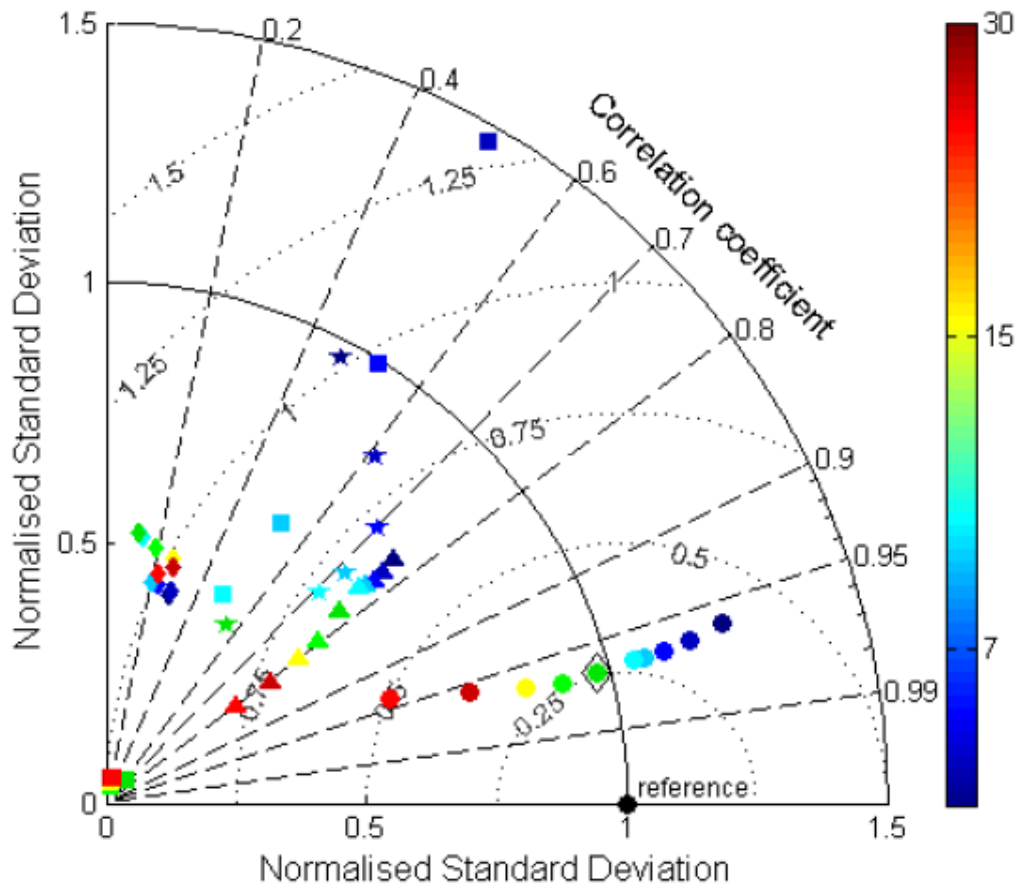


Figure 11. Taylor diagram for the model sensitivity to the vertical turbulent exchange parameterisation (different values of k_{min} are used) showing model to reference statistics for the oxygen (denoted with circles “●”), phosphorus (denoted with triangles “▲”), ammonium (asterisks “*”), nitrate (diamonds “◆”) and chlorophyll a (squares “■”) fields for the period 1998-2003 at BY5. The colour bar represents 10 different values of $k_{min} \cdot 10^7$ in the interval [5; 30]. The minimum value of the RMSD for oxygen is indicated by black diamond (“◇”).

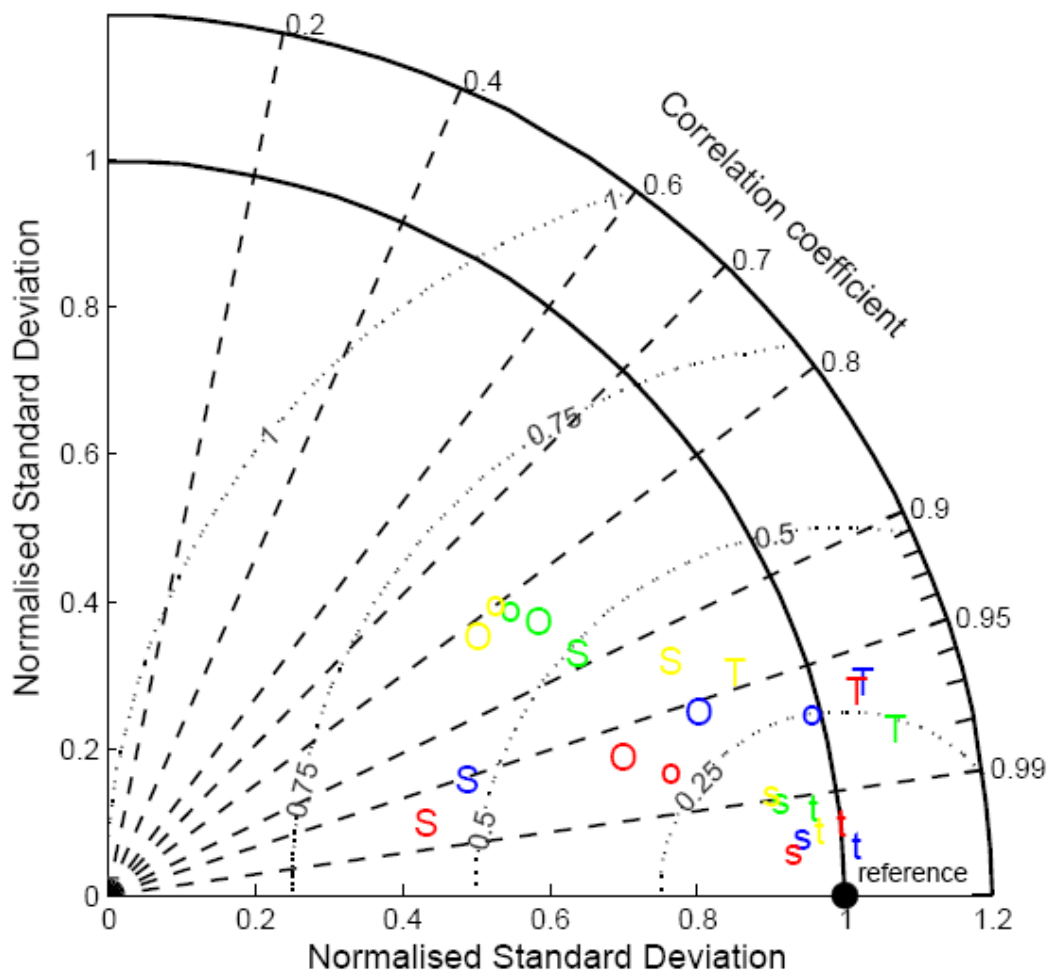


Figure 12. Comparison between the normalised pattern statistics of oxygen calculated for the period 1998-2003 from two separate model executions with different profiles used for temperature/salinity relaxation. With capital letters are denoted the comparison points obtained by using model 3D temperature/salinity fields for relaxation and with small letters those obtained by using observation data of BED (reference). The statistics for different stations are presented with different colours: Bornholm – blue; Gotland – red, Arkona – green; Fladen – yellow.

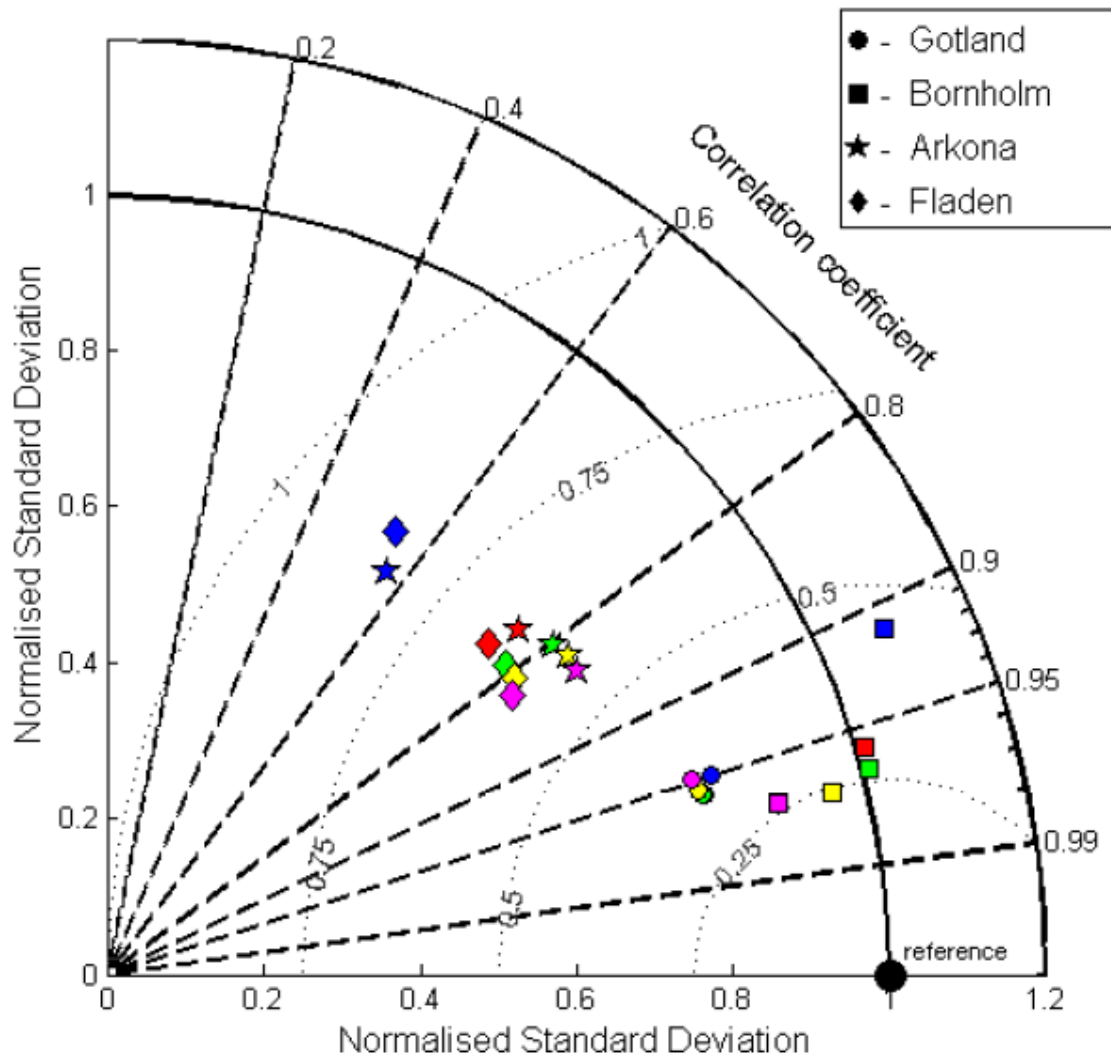


Figure 13. Normalised pattern statistics of oxygen at the principal stations for the period 1998-2003. Different colours represent model executions with different wind speed scaling: 0.5 – blue; 0.8 – red; 1.0 – green; 1.2 – yellow; 1.5 – magenta.

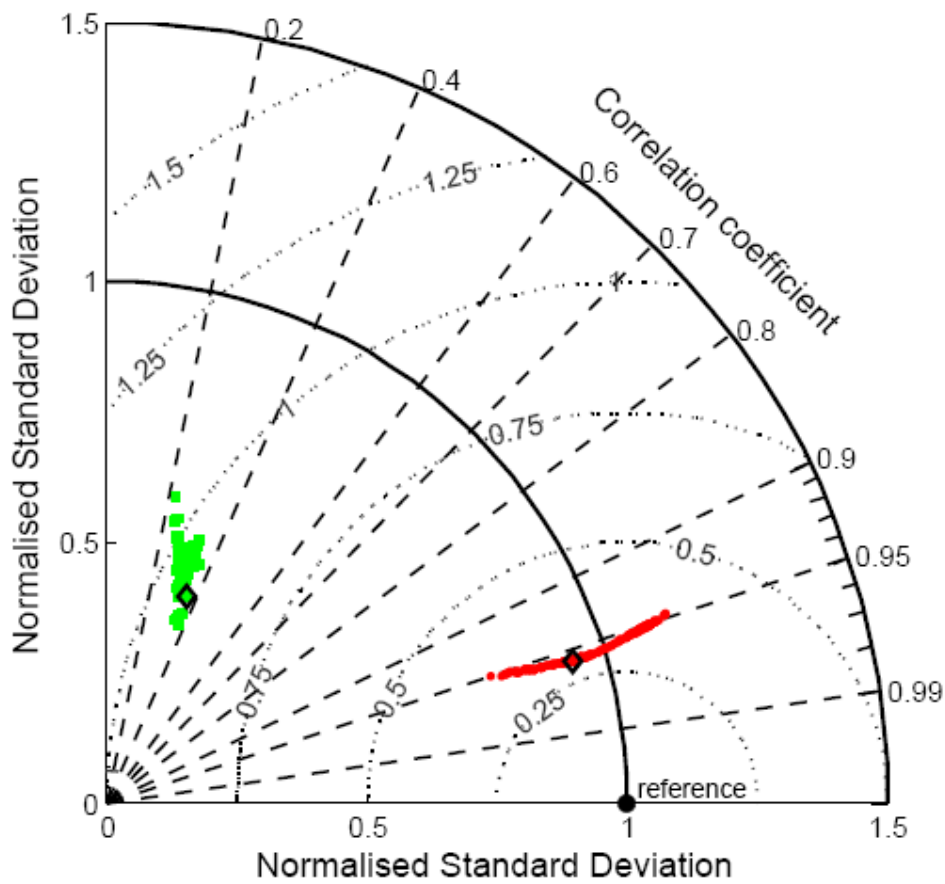


Figure 14. Taylor diagram for model sensitivity to limiting nutrients showing model to reference statistics for the oxygen (red) and the chlorophyll a (green) field for the period 1998-2003 at BY5. The comparison points with the minimum RMSD values are indicated by black diamond (“◊”). The ranges of the intervals in which vary the initial concentrations and surface fluxes of nutrients are given in Table 4.